



# Batteries Safety: Recent Progress and Current Challenges

Teyeb Ould Ely<sup>1\*</sup>, Dana Kamzabek<sup>2</sup> and Dhritiman Chakraborty<sup>3</sup>

<sup>1</sup> Department of Chemical Engineering, University of California, Santa Barbara, Santa Barbara, CA, United States,

<sup>2</sup> Department of Chemistry, School of Science and Technology, Nazarbayev University, Astana, Kazakhstan, <sup>3</sup> Warwick Centre for Predictive Modelling, School of Engineering, University of Warwick, Coventry, United Kingdom

## OPEN ACCESS

### Edited by:

Qingsong Wang,  
University of Science and Technology  
of China, China

### Reviewed by:

Huan Pang,  
Yangzhou University, China  
Hailei Zhao,  
University of Science and Technology  
Beijing, China

### \*Correspondence:

Teyeb Ould Ely  
ouldely00@ucsb.edu

### Specialty section:

This article was submitted to  
Electrochemical Energy Conversion  
and Storage,  
a section of the journal  
Frontiers in Energy Research

**Received:** 02 February 2019

**Accepted:** 12 July 2019

**Published:** 25 September 2019

### Citation:

Ould Ely T, Kamzabek D and  
Chakraborty D (2019) Batteries Safety:  
Recent Progress and Current  
Challenges. *Front. Energy Res.* 7:71.  
doi: 10.3389/fenrg.2019.00071

In this growing age of clean energy and the use of power storage to circumvent the use of traditional fossil fuel technologies, batteries of greater capacity, storage, and power are increasingly becoming indispensable. New chemistries are being developed to increase the capacity of traditional lithium ion batteries and to develop batteries beyond Lithium ion. Promising high capacity cathodes and anodes are developed however their large-scale deployment is hindered due to safety concerns. In this review, we summarize recent progress of lithium ion batteries safety, highlight current challenges, and outline the most advanced safety features that may be incorporated to improve battery safety for both lithium ion and batteries beyond lithium ion. Of particular interest is the issue of thermal runaway mitigation by incorporation of novel nano-materials and advanced technologies.

**Keywords:** lithium ion batteries, batteries safety, thermal runaway, smart separators, lithium dendrites suppression, electrolyte safety, structured current collectors

## HIGHLIGHTS

This review provides a bird's-eye view of most recent LiB batteries failure mechanisms and classifies them by their relevance to each battery component. The review highlights critical challenges associated with each failure mitigation approach and discusses them with regard of recent literature in a short, concise and critical manner. The review also highlights the two most promising future research directions in the field of battery safety: (1) aqueous batteries with expanded electrochemical window of stability, (2) all solid state batteries with low interfacial impedances. These two research areas guided by recent advanced diagnostic tools and computational predictive models will enable safer future high capacity storage systems.

## INTRODUCTION

Lithium ion batteries are composed of an anode that is typically graphite and a cathode that is typically an intercalated lithiated oxide, submerged in a liquid electrolyte, and separated by a polymer separator [polypropylene (PP) or polyethylene (PE)]. The active electrode materials (anode/cathode) are usually coated on a current collector (Cu, Al foil). Most batteries have some additional components such as battery management systems, safety devices, tabs and a cover as described **Figure 1**.

The discovery of lithium insertion in graphite can be traced back to the work of Herold (1955), 10 years later (1965) LiC<sub>6</sub> is synthesized using non-electrochemical processes (Juza and Wehle, 1965). The concept of rocking chair battery where lithium shuttles (rocks) between two electrodes

is formulated by Armand in the late seventies (Armand, 1980) and proven experimentally using lithiated tungsten dioxide and titanium disulfide as an electrode (Besenhard and Eichinger, 1976; Eichinger and Besenhard, 1976; Lazzari and Scrosati, 1980). The outstanding work of Yazami and Touzain (1983) led to the first practical use of graphite as an anode for secondary lithium ion batteries (LiB). While, the work of Mizushima et al. (1980) led to positive 4 V intercalation lithiated cathode oxides. The work of Yazami and Goodenough was instrumental in enabling Yoshino to invent and formulate the structure of lithium ion battery as we know it today (Yoshino, 2012). Yoshino solved some major technical challenges such as lowering the internal resistance of the battery and enabling efficient use of liquid electrolytes. SONY developed Yoshino's cell further and commercialized it in the early 1991. A historical account of major breakthroughs that led to the discovery of lithium ion batteries is provided in **Table 1**.

Nowadays, lithium ion batteries dominate the market of portable electronics and count for almost one quarter of all batteries produced worldwide. In Japan alone, rechargeable batteries represent 39% of the total battery production with high capacity lithium ion representing more than 50% of rechargeable batteries (**Figures 2A,B**). The production of lithium ion batteries is forecasted to increase exponentially in the upcoming decade due to their large-scale integration in public transportation, autonomous vehicle, drones, aerospace, military, and medical sectors (**Figure 2C**).

Extensive adoption of LiB in transportation is still hindered by their short range, high cost, and poor safety.

To overcome these challenges, LiB pack system should be defect free, have an energy density of 235 Wh kg<sup>-1</sup> or 500 Wh L<sup>-1</sup>, and should be dischargeable within 3 h. In addition, the LiB battery pack should have a cyclability of more than 1,000 cycles with a calendar life of up to 15 years. However, most lithium ion batteries available on the market today do not satisfy these requirements, in particular safety concerns are still one of the main hurdles facing large scale adoption of lithium ion batteries in public transportation.

In the civil aviation transportation sector alone more than 225 incidents involving LiB are reported (FAA Office of Security Hazardous Materials B. B.-P. D, 1991).

One of the most notable aviation safety incidents happened on the 16th of January 2013 when the entire fleet of Boeing 787,

the much touted "Dream Liner" was grounded by the US Federal Aviation Administration (FAA). As was revealed by the NTSB investigation, the fault lays in the Lithium Ion Batteries (LiB) used to power the onboard apparatus of the plane<sup>1</sup> (Mark, 2014). An internal short circuit instigated fire and smoke in a single cell of the Auxiliary Power Unit (APU) Lithium ion Battery LiB and cascaded to the adjacent cells. The root cause of this internal short circuiting is unknown, however the presence of wrinkles and mechanical abnormalities in the windings processes could have resulted in uneven charging of the anode causing lithium deposition and subsequent thermal runaway.

Lithium ion battery safety concerns affects other transportation sectors; the US government's auto safety watchdog has opened several investigations into battery fires in electric vehicles (Klayman and Bernie, 2013). External mechanical abuse (such as nail penetration and mechanical deformation as a result of electric vehicle collision) compromise LiB cell safety and lead to fire and explosion. Similarly, electrical abuse as a result of overcharge/overdischarge can compromise batteries safety (Feng et al., 2018).

In terms of portable electronic devices, countless incidents are reported, and the most notable being the failure of Samsung Galaxy 7 in 2017, and the subsequent financial loss of 17 billion dollars (Loveridge et al., 2018). As we will discuss in more detail in the separator safety section, manufacturing defect of the separator is the primary factor behind thermal runaway and failure of Samsung Galaxy 7.

Furthermore, between 2009 and 2016 at least 195 fires and explosion linked to LiB in electronic cigarettes<sup>2</sup>, and 60 fires related hoverboards are reported. These incidents and many more triggered intense interest in batteries safety research<sup>3</sup>. The focus of this research is primarily on improving the stability of the electrode, the electrolyte and the separator materials.

In this review, we discuss lithium ion batteries safety: state of the art and current challenges. The review is divided into eight main sections. After a general introduction in the first section, we address, in the second section, the concept of thermal runaway and its triggering factors. In the third section, we address thermal runaway in multicell pack. Beside electrode degradation the root cause of most thermal runaway phenomena is dendrite formation, thus section four addresses advanced strategies to mitigate dendritic growth of lithium. The challenges facing the development of safe electrode materials will be discussed in the fifth section, while those facing the electrolytes safety and the separators will be presented in the sixth and seventh sections, respectively. In the eighth section, we review the role of current collectors in battery safety and thermal runaway mitigation. We conclude each section by a foray into novel materials and chemistries and their potential uses to mitigate thermal runaway.

**Abbreviations:** AMPip-TFSI, 1-allyl-1-methylpiperidinium bis(trifluoromethanesulfonyl)imide; APU, Auxiliary Power Unit; ARC, Accelerating Rate Calorimetry; BMP-TFSI, Butylmethylpyrrolidiniumbis(trifluoromethylsulfonyl)imide; BMS, Battery Management System; C/E, Capacity/Energy; CID, Charge Interrupt Devices; DMTP, 1,1,1,2,2,3,4,5,5,5-decafluoro-3-methoxy-4-(trifluoromethyl)-pentane; DSC, Differential Scanning Calorimetry; DVD, Digital Versatile Disc; EV, Electric Vehicle; FAA, Federal Aviation Administration; FEC, Fluoroethylene Carbonate; FP, Flash Point; GO, Graphene-Oxide; LATP, Li<sub>1+x</sub>Al<sub>x</sub>Ti<sub>2-x</sub>(PO<sub>4</sub>)<sub>3</sub>; LiB, Lithium Ion Batteries; LLZO, Li<sub>7</sub>La<sub>3</sub>Zr<sub>2</sub>O<sub>12</sub>; LMO, Lithium-Manganite; LPS, Li<sub>2</sub>S-P<sub>2</sub>S<sub>5</sub>; LTAP, Li<sub>1+x+y</sub>Al<sub>x</sub>Ti<sub>2-x</sub>Si<sub>y</sub>P<sub>3-y</sub>O<sub>12</sub>; LTO, Lithium Titanate Li<sub>4</sub>Ti<sub>5</sub>O<sub>12</sub>; PE, Polyethylene; PI, Polyimide; PMMA, Poly(methyl methacrylate); PP, Polypropylene; PTC, Positive Temperature Coefficient; SE, Solid Electrolyte; SEI, Solid Electrolyte Interphase; SEM, Scanning Electron Microscopy; SOC, State-of-Charge; TBBA, Tetrabromobisphenol A; TEM, Transmission Electron Microscopy; CNT, Carbon Nanotubes; NTSB, National Transportation Safety Board; CE, Coulombic Efficiency; LiFOB, Lithium Difluoro bis(OxalatoBorate).

<sup>1</sup><https://www.nts.gov/investigations/AccidentReports/Reports/DCA13IA037-interim-factual-report.pdf>

<sup>2</sup>[https://www.usfa.fema.gov/downloads/pdf/publications/electronic\\_cigarettes.pdf](https://www.usfa.fema.gov/downloads/pdf/publications/electronic_cigarettes.pdf)

<sup>3</sup><https://www.cnn.com/2016/07/06/health/hoverboard-recall-fire-hazard/>

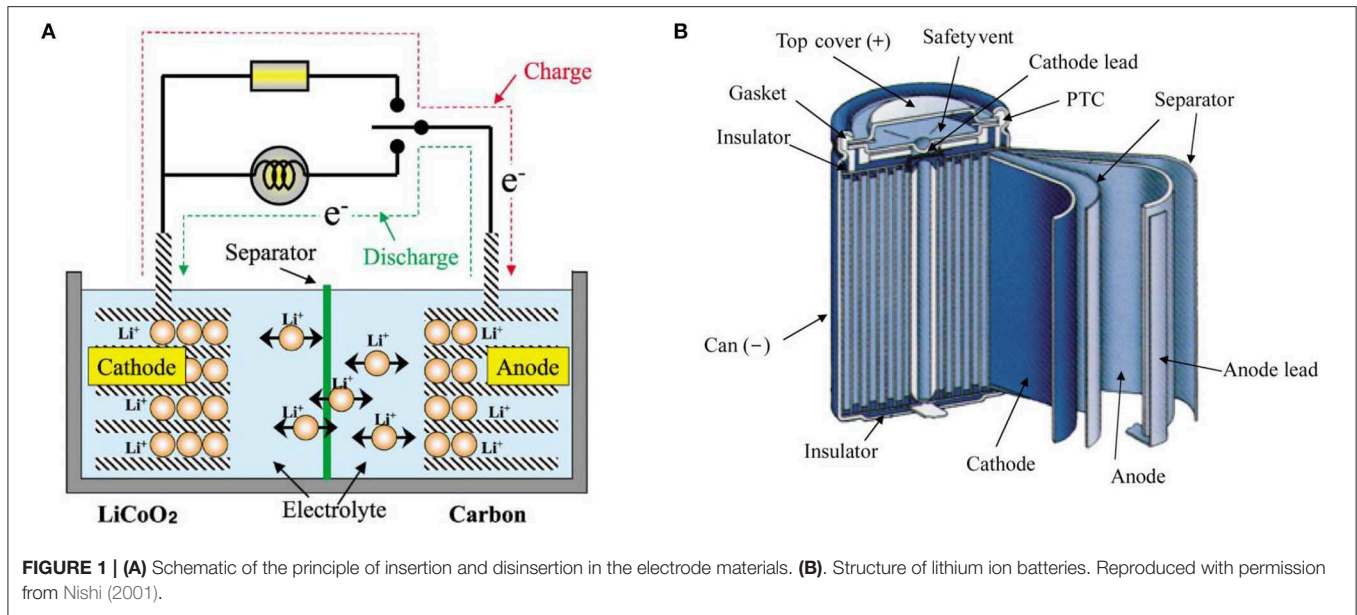


**FIGURE 1 | (A)** Schematic of the principle of insertion and disinsertion in the electrode materials. **(B)** Structure of lithium ion batteries. Reproduced with permission from Nishi (2001).

**TABLE 1 |** Historical account of the major breakthroughs in lithium ion batteries discovery.

Date	References	Breakthroughs
1955	Herold, 1955	First report of the lithium insertion in graphite by non-electrochemical processes
1965	Juza and Wehler, 1965	First synthesis of LiC <sub>6</sub> by electrochemical processes
1970	Armand, 1980	First formulation of the idea of the rocking chair battery, where lithium shuttles between the two electrodes
1980	Lazzari and Scrosati, 1980	First experimental implementation of the idea of rocking chair battery using lithiated tungsten dioxide and titanium disulfide as an electrode.
1980	Mizushima et al., 1980	First discovery of lithiated transition metal oxides that reversibly deintercalate/reintercalate lithium. One of these oxides (LiCoO <sub>2</sub> ) was commercialized by Sony's in 1991
1981	Hunter, 1981	First discovery of MnO <sub>2</sub> (λ-form), with a spinel structure, that can reversibly be reduced and oxidized in organic electrolytes at a high potential similar to that of LiCoO <sub>2</sub> with a similar capacity. The MnO <sub>2</sub> (λ-form) was commercialized later
1983	Yazami and Touzain, 1983	The world first demonstration of lithium insertion and release from graphite leading to practical use of graphite as an anode for secondary lithium ion battery. Yazami's cell displayed high internal resistance due to the use of polymer electrolyte and was destined to fail with some liquid electrolytes.
1985	Sanechika and Yoshino, 1985; Yoshino, 2012	Investigation and description of the benefits of low temperature carbons such as petroleum coke. The use of practical liquid electrolytes and the construction of the first operational high capacity LIB at Asahi Kasei. The LIB battery was ultimately developed (Nishi, 2001) and commercialized by SONY in 1991.

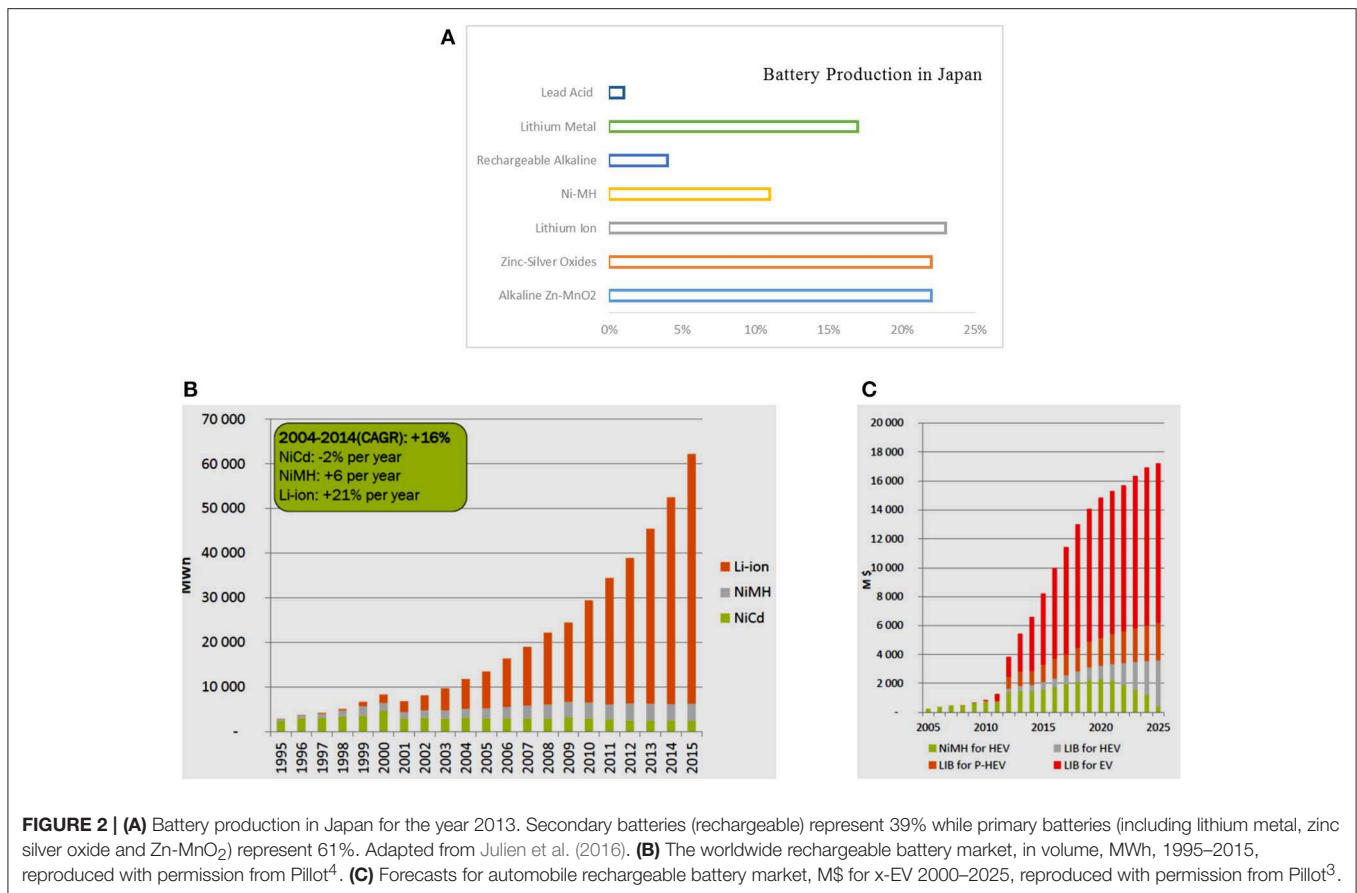
## THERMAL RUNAWAY?

Thermal runaway is a phenomenon that occurs in batteries as a result of heat generating exothermic reactions inside the battery, raising the temperature further and potentially causing more failure or explosion.

The temperature at which thermal runaway is likely to occur varies from 130°C to well over 250°C depending on the cell configuration (i.e., size, design, and electrode materials). Most safety problems can be mitigated prior to thermal runaway onset temperatures. However, once thermal runaway starts the cell temperature increases irreversibly causing further degradation of the cell components (cathode breakdown, electrolyte breakdown, and separator meltdown). Under these conditions, the rate of heat generating reactions exceeds the cell capacity of heat dissipation (Wang et al., 2010, 2012), causing the battery to heat up, catch fire and explode.

The causes of thermal runaway vary depending on the cell chemistry involved. It turned out that internal short can trigger thermal runaway but is only responsible for a small fraction of the heat generating processes. In cells where the cathode is Li(Ni<sub>x</sub>Co<sub>y</sub>Mn<sub>z</sub>)O<sub>2</sub>, the main causes of heat generation are the redox reactions between the anode and the cathode (Feng et al., 2019). Thus, from safety perspective, it would be advantageous to develop a chemistry that minimizes the exothermicity of contact redox reactions between the anode and the cathode.

Oxygen resulting from the cathode degradation reacts exothermically with both the anode and the electrolyte accelerating further degradation. To mitigate oxygen release, several new strategies are suggested and reviewed elsewhere (Sharifi-Asl et al., 2019). Among these strategies, doping is widely investigated as it improves structural stability of the cathode. Inactive dopants remain in Li slabs of lithiated



cathode acting as pillars that improve the overall structural stability of the cathode. Furthermore, large size dopants increase the spacing between the layers and provide Li ion with fast diffusion pathways with low activation energy. Other strategies to mitigate oxygen release and cathode degradation upon cycling include chemical gradient design and core-shell coating (Sharifi-Asl et al., 2019).

Most batteries operate safely in a window from 0 to 60°C. At low temperatures (< -10°C) there is low charge transfer due to high electrolyte viscosity and increased risk of Lithium plating. For temperatures between 60 and 120°C, the main risk is a breakdown of the SEI layer. These risks may be mitigated by BMS/current shut off. At high temperatures of around 120°C, the separator starts to degrade and melt. This leads to internal short circuits and gas emissions from the electrolyte. However, the risk may still be contained and mitigated by using cell vents to release the pressure buildup and shut off the current. At even higher temperatures over 180°C there is permanent damage to cell components including the cathode, anode or electrolyte leading to thermal runaway. At this point it is too late to prevent cell degradation and destruction.

Besides physical abuse of the cell, thermal runaway can be triggered by electrical abuse such as over-charge/over-discharge

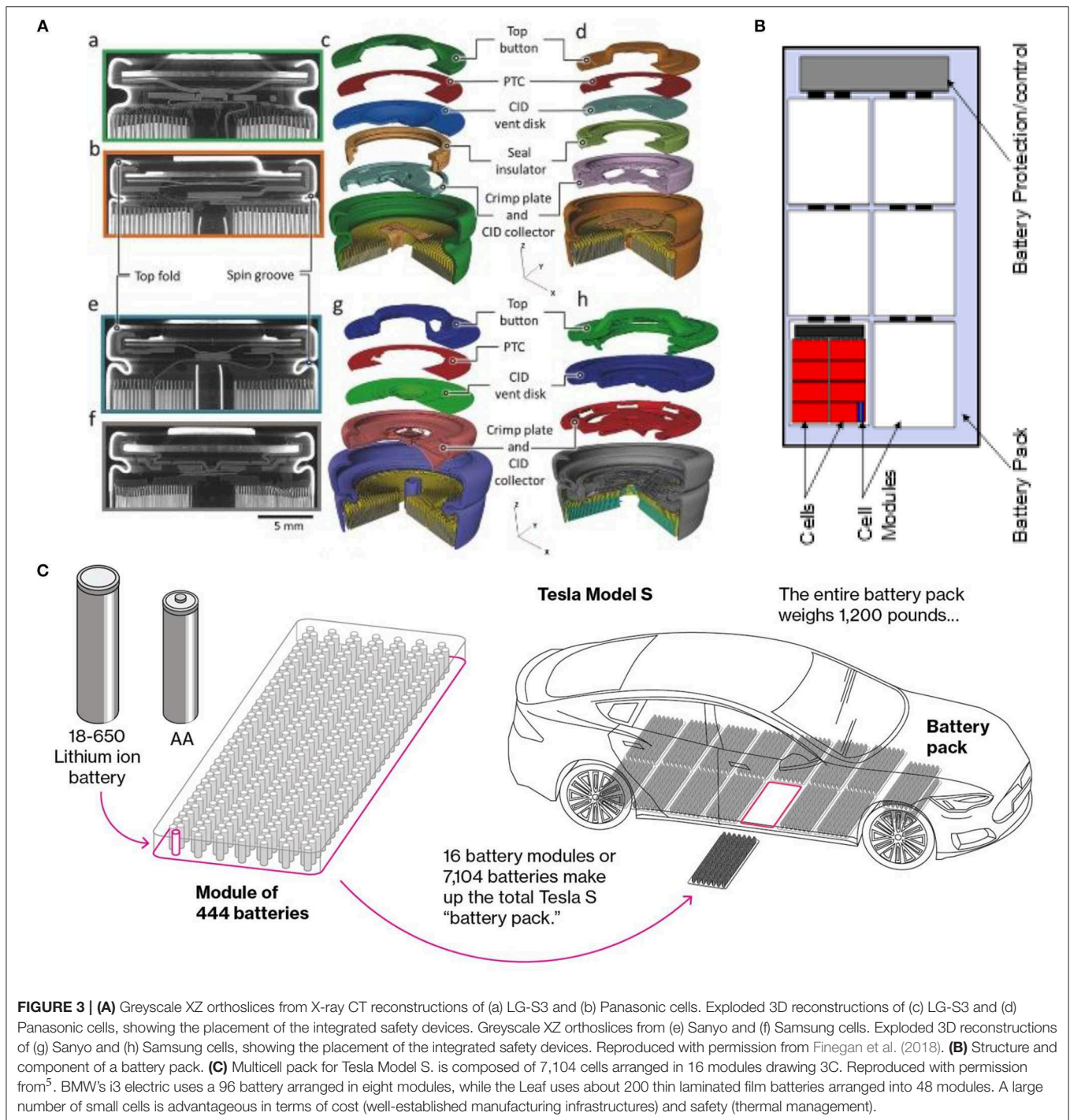
(i.e., charge/discharge above/below the manufacturer's high/low voltage specification). Under electrical abuse the cell experiences rapid heating due to abnormal current flow and leading to thermal runaway.

Safety measures such as PTC devices, fuses and BMS detect external shorts, turn-off the current and disable the cell. Polyethylene blended with a conductive filler (typically carbon black) is typically used for PTC applications. This composite changes its resistance with heat and is often placed in the cap. Once activated, the battery remains in a tripped state until the source of external short is cleared (Pesaran et al., 2008). Furthermore, separators composed of multilayer with variable phase transition temperatures can shut down the cell and prevent excessive internal heat. As the temperature increases, the layer with low phase transition temperature melts and shuts down the pores of the solid layers, stopping ion transport and current flow disabling the battery (Li et al., 2018).

In addition to PTC, separator and BMS component, commercial LiB are equipped with Charge Interrupt Devices (CID) and safety vents that open in response to an increase in the internal battery pressure. These safety devices are usually placed in the cell cap (see Figure 3A).

CID is a pressure valve that acts as an overcharge protection device and disables the cell permanently if its internal pressure is too high (>145 psi). CID activation can be triggered by electrolyte breakdown and/or significant battery over-discharge/overcharge incidents (Celina et al., 2011).

<sup>4</sup>[http://www.avicenne.com/pdf/Fort\\_Lauderdale\\_Tutorial\\_C\\_Pillot\\_March2015.pdf](http://www.avicenne.com/pdf/Fort_Lauderdale_Tutorial_C_Pillot_March2015.pdf)



## THERMAL RUNAWAY FROM CELL TO PACK

Single cell batteries are usually packed into a multi-cell pack organized in a module and connected to a pack protection and controls system (Figure 3B). The number of cells varies

depending on the pack voltage and capacity requirements. Battery packs for electric vehicles are usually composed of thousands of single cells (Figure 3C). Numerous safety incidents show that a thermal runaway initiates in a single cell and propagates to other cells in the pack. A thermal runaway is an extremely fast process that occurs at a time scale  $<2$  s, leading in most cases to battery rupture in less  $<0.01$  s. Ultra-high-speed synchrotron X-ray imaging elucidated the failure

<sup>5</sup>[https://www.mpoweruk.com/lithium\\_failures.htm](https://www.mpoweruk.com/lithium_failures.htm) (accessed July, 3, 2019).

processes of most common 18,650 commercial cells undergoing thermal runaway. The failure mechanism is mostly due to a poor venting process that leads to an extreme internal pressure, causing the electrode assembly to shift and further clog the vent opening, causing the cell rupture. To mitigate this problem, the incorporation of an additional vent at the base of the cell alongside with robust casing are recommended (Finegan et al., 2015, 2018).

Thus, one dysfunctional cell can cause damage to the entire pack, and therefore, it is important to isolate the damaged cell and create pathways for heat dissipation. External lateral heat transfer is the primary mechanism of thermal runaway migration to the adjacent cells (Spotnitz et al., 2007; Feng et al., 2015). Enlarging the space between cells (Lopez et al., 2015; Zhong et al., 2018) and creating thermal conducting pathways to dissipate heat are the most effective strategies to isolate the dysfunctional cell. Heat dissipation can be performed using either active air cooling with finned heat spreader, passive air cooling, liquid cooling conduits, refrigerant cooling with cold plate, or liquid cooling with heat exchange plate (which is mostly employed in EV batteries). The weight, volume and cost of these strategies led to the development of light weight, low cost, and graphite-based heat spreaders that are 28% lighter than aluminum (Beyerle et al., 2013).

Furthermore, aluminum foam with small porosity is found to be an excellent heat sink, to lower surface temperature of the battery module and improves its friction factor (Figure 4) (Saw et al., 2017).

The voltage of lithium-ion batteries is commonly managed by an external electronic circuit with the sensors connected to each individual cell of the battery pack. The battery management system (BMS) is required to prevent state-of-charge (SOC) and capacity/energy (C/E) mismatch. The BMS is usually designed to keep the battery in a safe voltage range, prevent thermal runaway cascading, release overpressure and dissipate heat. The vast majority of commercial LiB can be operated safely between 3.0 and 4.2 V, with a “nominal” voltage around 3.6–3.7 V. Discharge below this nominal voltage can damage the electrodes while charging above 4.2 can lead to rapid exothermic degradation followed by thermal runaway and explosion. It is, therefore, advisable to charge the cells within the limits that are usually specified by the manufacturer. Some specialty batteries enable safe discharge to zero Volts without causing permanent damage to the cell (Tsukamoto et al., 2015).

Physical deformation of a single cell in a pack can be a precursor of short-circuiting as have recently been suggested by computational modeling (Wang et al., 2019).

The advent of machine learning and big data centers is expected to improve batteries management systems and safety. Remote battery monitoring centers linking BMS with big data facilities is already suggested (Figure 4B) (Xiong et al., 2018).

## THE CHALLENGE OF LITHIUM DENDRITES

Dendritic growth of lithium is one of the main internal mechanisms by which LiB cells fail. Lithium dendrite induce an internal short and impede large scale adoption of Li-air

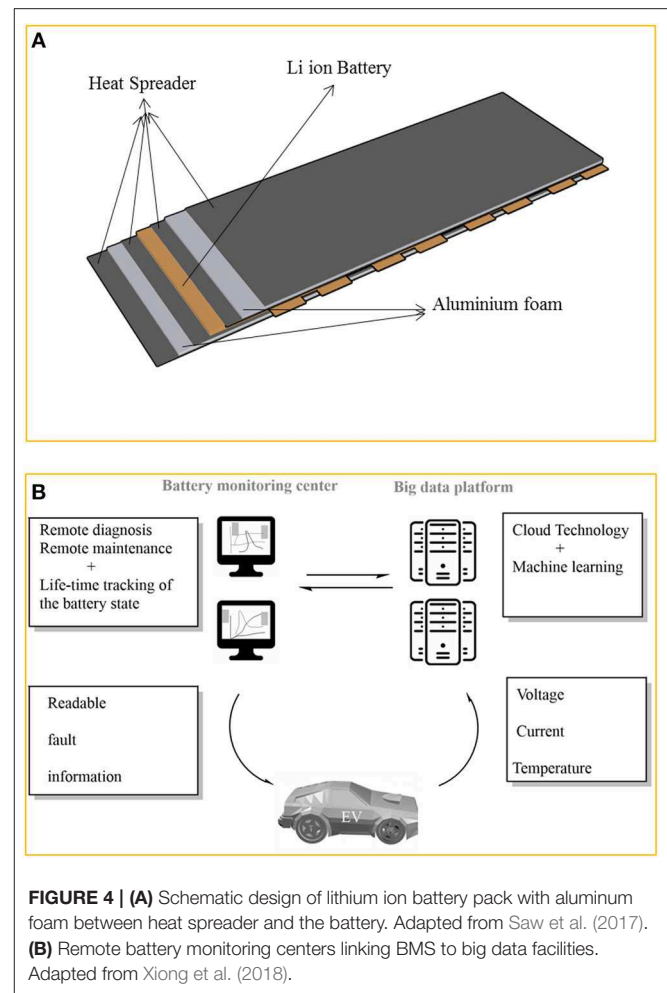


**FIGURE 4 | (A)** Schematic design of lithium ion battery pack with aluminum foam between heat spreader and the battery. Adapted from Saw et al. (2017). **(B)** Remote battery monitoring centers linking BMS to big data facilities. Adapted from Xiong et al. (2018).

and Li-sulfur batteries. Dendrites grow from the anode and penetrate the polymer separator which consequently leads to short-circuiting when it reaches the cathode (Aurbach et al., 2000; Mark, 2014). Short-circuiting, accelerates exothermic reactions between the electrodes and the flammable organic electrolytes leading to fire and explosions. An understanding of dendritic pattern formation at the nanoscale may enable prevention of lithium dendrite growth.

Recent work using TEM liquid cells reveals that dendritic growth of metal oxides proceeds by crystal splitting mechanism (Hauwiller et al., 2018). The latter is promoted by stacking fault and dislocations (Kelly et al., 2007) that are produced by inhomogeneities or impurities in the growth medium. The facets of the growing crystal split along the stacking fault and dislocations lines (Ould-Ely et al., 2006; Rusakova et al., 2007) and compete for the solute. These observations are in agreement with dendritic crystal growth theories (Mullins and Sekerka, 1963) and the ligand capping theory (Liao et al., 2014).

Experimental studies show that lithium dendrites can be suppressed by four main mechanisms: (1) additive with strong capping abilities (Li et al., 2015; Zhang et al., 2019), (2) lithiophobic coating (Kozen et al., 2015; Lee et al., 2017;

Zhang et al., 2017a) that can redirect the growth away from the separator, and (3) confinement and encapsulation in pre-patterned or porous structures (Yan et al., 2016; Chi et al., 2017), and (4) the use of solid state electrolytes.

### Dendrites Suppression by Additives

Development of an electrolyte or solvent system that strongly bind on the facets of lithium growing crystals is a viable strategy to interdict dendritic growth (Li et al., 2015). It was discovered that the addition of organic and inorganic substances into an electrolyte solvent can positively affect the stability of the SEI layer and suppress dendrite growth.

Cui and co-workers manipulated the concentrations of  $\text{Li}_2\text{S}_8$  and  $\text{LiNO}_3$  additive to prevent lithium dendrites and achieve Coulombic efficiency of  $\sim 99\%$  over 300 cycles (Li et al., 2015) at a practical current density of  $2 \text{ mA cm}^{-2}$  and areal capacity of  $6 \text{ mAh cm}^{-2}$ .

Researchers from Tsinghua University reported that fluoroethylene carbonate (FEC) additives retard dendrite growth on Li anode side (Zhang et al., 2017b). According to this work, FEC reacts spontaneously with lithium and produces LiF that contributes to the growth of a stable LiF-rich SEI layer.

Furthermore, LiF is an electrical insulator that prevents electrons from crossing the SEI layer at the same time, it promotes ionic conductivity of lithium ions reducing the chances of polarization and lithium dendrite formation. The net result of these attributes is an improved coulombic efficiency with excellent cyclability (CE: 98% within 100 cycles) (Kozen et al., 2015).

Another smart solution is the use of non-Li cations as an electrolyte additive. Increasing concentrations of these cations' additives lead to the formation of a positively charged electrostatic region. This effectively creates a cation shield that reduces the formation of dendrites in cells (Ding et al., 2013). Cations possessing effective reduction potential lower than Li standard reduction potential (e.g., cesium, rubidium) are deposited selectively on the surface of a growing dendrite, and electrostatically shield it from additional  $\text{Li}^+$  ions; hence lithium starts to accumulate on the neighboring regions resulting in suppression of dendrite growth. However, the adsorbed additive cations should remain oxidized to prevent their incorporation in the SEI layer. In addition to forming stable and regular SEI layer that suppress dendrite growth the solvation sheath of lithium ions need to be carefully controlled (Zhang et al., 2019).

One main disadvantage of additives is their potential interference with ionic conductivities of electrolytes since considerable amount of additive is usually required to ensure optimal SEI layer.

### Dendrites Suppression by Lithiophobic/Lithiophilic Coating

Lithium dendrite growth can be manipulated by lithium metal surface coating and modification (Kozen et al., 2015; Lee et al., 2017; Zhang et al., 2017a). Lithium fluoride (Xie et al., 2017), lithium nitride (Li et al., 2015), polymers (Liang et al., 2015; Liu et al., 2016), and carbon-based coating (Huang et al., 2017) have been used to regulate SEI layer and suppress dendritic growth.

Lithium wettability of various substrates proved that some lithiophobic substrates are efficient in inhibiting dendritic growth (Yan et al., 2016; Chi et al., 2017). One such substrate is silver (20 nm thick) coated carbon cloth that is shown to redirect lithium dendritic needles away from the separator and reduces the risk of short-circuiting (Tian et al., 2018). The main drawback of silver coating beside its cost is its possible corrosion upon contact with various electrolytes.

Another strategy consists of coating lithium metal with lithiophilic–lithiophobic gradient interfacial bilayer composed of zinc oxides and carbon nanotubes (CNT). The lithiophilic zinc oxide sublayer bind to lithium foil while the lithiophobic CNT sublayer prevents dendrite formation. The “anchoring” provided by the zinc oxide sublayer promotes and stabilizes SEI layer while preventing the formation of a corrosion layer. The top CNT layer effectively suppresses dendrite growth and enables lithium striping (Zhang H. et al., 2018) removed.

### Dendrites Suppression by Confinement

The encapsulation of lithium metal in a 3D scaffold is found to reduce the risk of thermal runaway and eliminate the risk of dendritic growth (Yan et al., 2016; Chi et al., 2017). As we will discuss in detail in section Separator Degradation and Safety, increasing the porosity of ceramic separators prevents lithium dendrite growth and penetration. This is due to the competition between the SEI layer formation within the pores and the dendritic growth, the latter ends up unfavorable due to the shape and cavities of the pores, leading to the formation of lithium whiskers (Bai et al., 2018).

Recently, perpendicular growth of Li-dendrites has effectively been suppressed upon using macroporous dendritic copper current collector (Umh et al., 2019).

### Dendrites Suppression Using Solid State Electrolytes

Solid electrolytes are efficient in suppressing dendritic growth of lithium. Dendrite growth in solid-state cells occurs as a result of a defect along the grain boundaries (Yu and Siegel, 2018) and surface cracks that create high local current density, leading to lithium electrodeposition and permeation through low shear modulus ceramic solid electrolytes.

To further shed light on the mechanism of the growth of dendrites on solid electrolyte surfaces, lithium electroplating on glassy LPS,  $\beta\text{-Li}_3\text{PS}_4$ , poly-, and single-crystal LLZTO, is investigated using galvanostatic electrodeposition (Porz et al., 2017; Swamy et al., 2018). Lithium infiltration resulting in short circuits occurred at a relatively slow time scale (minute time scale), current density relatively high ( $10 \text{ mA/cm}^2$ ) and initiated in the perimeter of the working electrode. See Figure 5.

Electric field amplification in the cracks and defects of the electrode drives lithium penetration from the perimeter of the working electrode to the solid electrolyte surface with supercritical surface flaws.

The high local current densities promote dendrites growth. The magnitude of these current varies as a function of the thickness-to-width aspect ratio of the cell and the size of the electrode. A large cathode with a smaller thickness to width

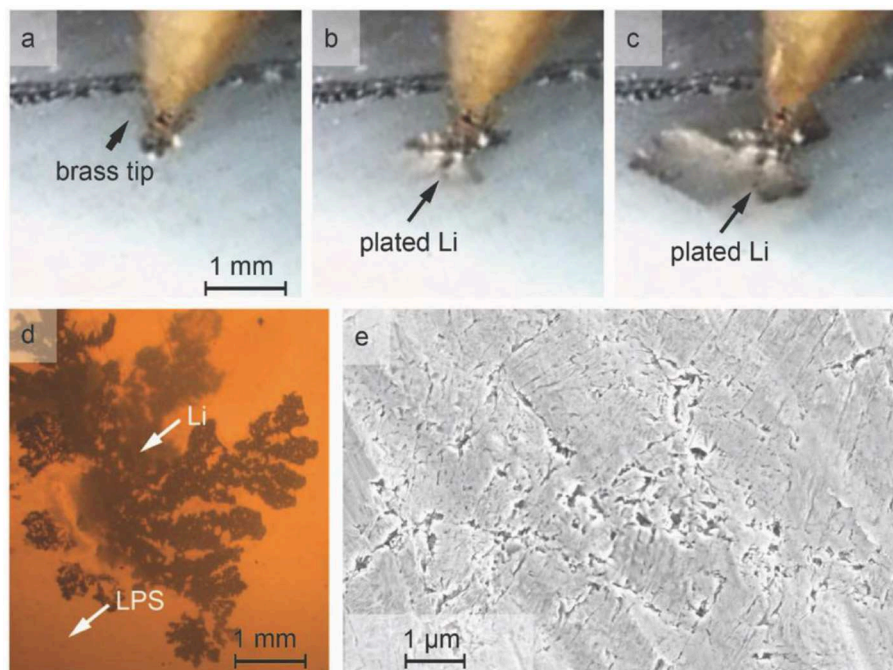


**FIGURE 5 | (a–c)** “Lithium metal deposition at high current density ( $\approx 50 \text{ mA cm}^{-2}$ ) propagates into densely pressed polycrystalline  $\beta\text{-Li}_3\text{PS}_4$  from a brass tip electrode. **(d)** Viewed in transmission optical microscopy, the lithium metal network shows a branching pattern. **(e)** The starting as-pressed surface of the  $\beta\text{-Li}_3\text{PS}_4$  polycrystal exhibits sub-micrometer ( $\approx 200 \text{ nm}$  length scale) cracks or pores.” Both figure and caption are reproduced with permission from Porz et al. (2017).

ratio compared to the anode promotes stronger lithium metal penetration (Swamy et al., 2018).

Furthermore, dendritic growth can be prevented using a solid electrolyte with a shear modulus 1.8 higher than lithium metal (Monroe and Newman, 2005). We will review solid electrolyte advantages in more detail in section Electrolyte Safety.

## SAFETY OF LIB ELECTRODE MATERIALS

### Current State of the Art

#### Anode Degradation and Safety Profile

One of the limiting factors of Li-ion batteries is the low capacity of their most common anode—the graphite. This led to the development of a new generation of higher capacity anodes based on metallic lithium, silicon, aluminum, germanium, and tin among others (Figure 6A). However, many of these high capacity anodes failed to replace the graphite due to pulverization and safety concerns.

The first successful graphite anode replacement was lithium-tin battery that was developed and marketed by SONY in 2005. This anode is based on the composite Sn/Co/C where Sn is the electro-active element. Incorporation of novel materials such as silicon nanomaterials and nanostructured graphene are also being actively considered (Guo et al., 2017; Mukanova et al., 2018).

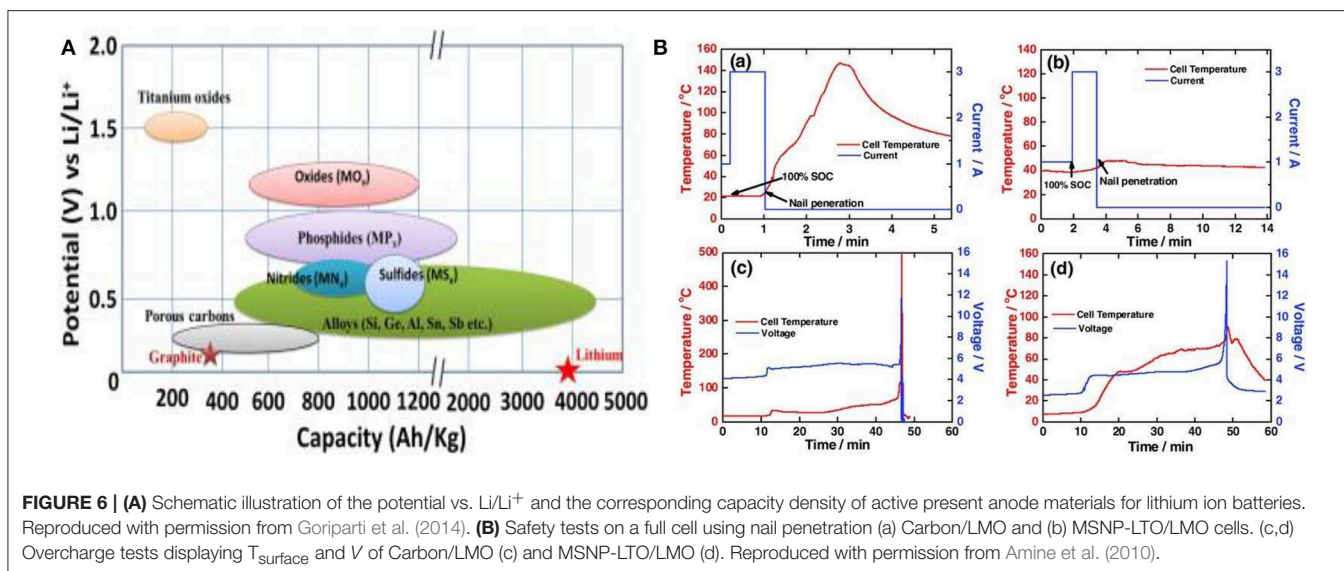
Owing to its high capacity, silicon is progressively replacing carbon based anodes. Novel graphite anode boosted with silicon coupled with a layered nickel (Ni)-rich lithium nickel manganese cobalt oxide cathode is already commercialized ( $\sim 270 \text{ Wh/kg}$ )

(Li et al., 2019). However, these silicon boosted cells suffer from  $\text{Li}^+$  loss into the thickened SEI layer, particle pulverization, and impedance rise (Li et al., 2019). Several start-up companies claim development of reliable silicon anode that can be integrated in EV batteries by 2023. The delay in commercializing these cells is due either to high cost, low performances and/or safety concerns.

Among the safest non-metallic anode reported so far,  $\text{Li}_4\text{Ti}_5\text{O}_{12}$  (LTO) displayed high resistance to pulverization as upon charging it expands only up to 16 vol% (Amine et al., 2010). LTO anodes have high operating voltage that excludes the growth of lithium dendrites and can intercalate up to three lithium ions in its spinel structure. Amine et al. (2010) successfully synthesized mesoporous LTO anode that displayed an excellent safety profile and passed both nail penetration and overcharge tests (Figure 6B).

Upon pairing  $\text{LiFePO}_4$  and  $\text{Li}_4\text{Ti}_5\text{O}_{12}$ , the cells displayed low specific energy of—only 50–60 Wh/kg. This energy level in LTO based anode is within the range of NiMH (45–75 Wh/kg) (Doughty and Roth, 2012).

In spite of its high cost and low natural abundance, Germanium (and its alloys) has been investigated as an anode for LiB. owing to its high storage capacity of  $1,384 \text{ mA h g}^{-1}$ , excellent lithium-ion diffusivity that is 400 times faster than silicon, and high electrical conductivity that is  $10^4$  times higher than silicon (Hu et al., 2016). Furthermore, Germanium has high rate capability as it can be cycled at a very high rate; up to 1,000 C (Graetz et al., 2004). Unfortunately, Germanium electrodes are known for poor cyclability due to their volume expansion and



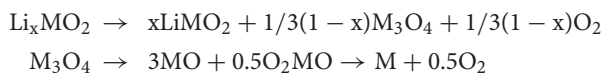
contraction that leads to electrode pulverization and detachment from the current collectors (Hu et al., 2016).

Anode materials based on metal oxides exhibit low capacities compared to metals and large potential hysteresis between the charge and discharge reactions and thus are unlikely to dominate the market of high capacity anode.

A comparative study of safety properties of most common anode materials is presented in **Table 2**.

### Cathode Safety and Degradation

The cathode end of lithium ion battery typically contains lithium ions that flow to the anode during the charging process. This positive electrode is usually made up of a transition metal oxide such as  $\text{LiCoO}_2$ ,  $\text{LiMn}_2\text{O}_4$ ,  $\text{LiFePO}_4$ ,  $\text{LiNiO}_2$ , and others. At elevated temperatures, these lithiated transition metal oxides are thermally unstable and release oxygen. The decomposition processes of lithiated cobalt oxide cathode materials are illustrated below



The oxygen generated can further react with non-aqueous solvents to produce more exothermic reactions. Extended periods of oxygen release may lead to fire hazards (Yazami and Touzain, 1983).  $\text{LiCoO}_2$  presents a risk of thermal runaway beyond  $155^\circ\text{C}$ , while batteries of  $\text{LiMn}_2\text{O}_4$  are stable up to  $180^\circ\text{C}$ .  $\text{LiNiO}_2$  is also unstable at high temperature ( $>150^\circ\text{C}$ ) and often Jahn-Teller distorted and contaminated with excessive nickel ions. The most important advantage of  $\text{LiNiO}_2$  is its high voltage compared to  $\text{LiCoO}_2$  (Kraytsberg and Ein-Eli, 2012).

In terms of cost and safety,  $\text{LiFePO}_4$  is the best cathode material and have been optimized and commercialized by A123 among others. However, its low specific capacity, poor conductivity ( $10^{-9}$  S/cm) and low lithium ion diffusion coefficient  $10^{-14}$   $\text{cm}^2/\text{s}$  are still major challenges.  $\text{LiMnPO}_4$  has low specific discharge capacities and rather poor rate capabilities

due to its low electronic ( $<10^{-10}$   $\text{S cm}^{-1}$ ) and ionic conductivity ( $<10^{-16}$   $\text{cm}^2 \text{s}^{-1}$ ). In addition,  $\text{LiMnPO}_4$  is structurally unstable and displays poor capacity retention, for these reasons it is not yet commercialized (Deng et al., 2017).

Thermal stability of most common cathode materials is given in **(Figure 7)**:

Cathodes based on  $\text{LiMn}_2\text{O}_4$  (LMO: specific capacity of 130 mAh/g) and  $\text{LiFePO}_4$  (LFPO; specific capacity of 140 mAh/g) are characterized by low energy density and good safety and rate capability. While cathode based on  $\text{LiNi}_{0.33}\text{Mn}_{0.33}\text{Co}_{0.33}$  (LNMC: specific capacity of 180 mAh/g) and  $\text{LiNi}_{0.80}\text{Co}_{0.15}\text{Al}_{0.05}$  (LNCA: 185 mAh/g) display high energy density and better safety profile than conventional  $\text{LiCoO}_2$  (LCO: 160 mAh/g).

### Novel Electrode Chemistries and Future Challenges

The most advanced and promising anode and cathode combination are highlighted in **Figure 8**.

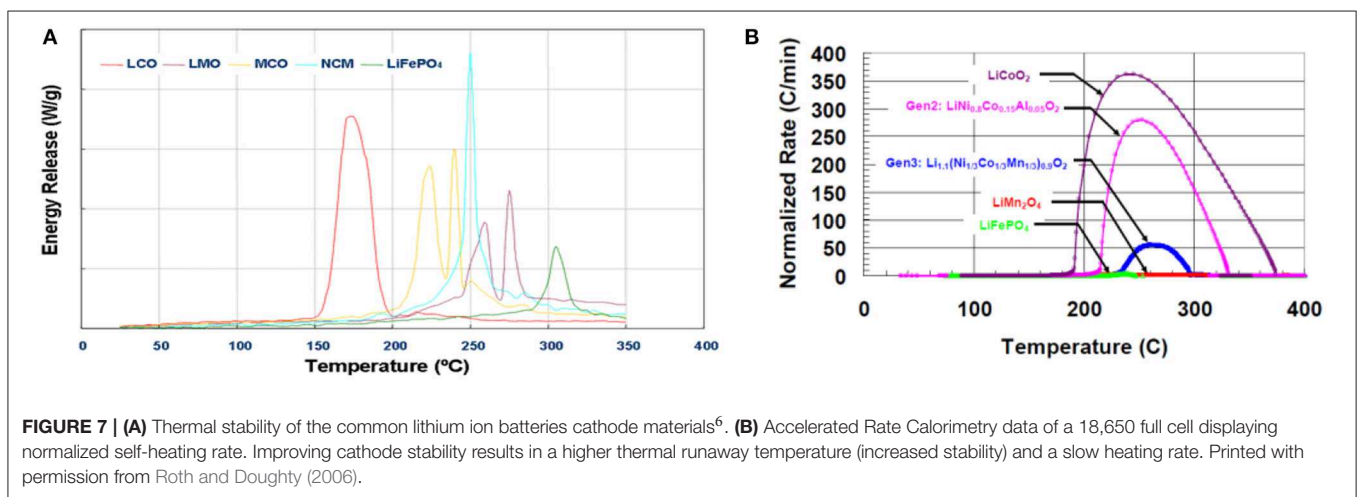
As stated earlier, in spite of its high safety Lithium Titanate (LTO) anode materials are not expected to dominate the EV market due to their low voltage. In contrast, an anode based on metallic silicon and lithium alongside with layered LNMC and sulfur for the cathode are expected to be part of future high capacity electrode materials. Panasonic and Hitachi Maxell-Kopin are already integrating small amounts of silicon (mostly as  $\text{SiO}_x$ ) to boost the capacity of graphite in their commercial LiB cells. However, these cells are not full proof against thermal runaway. Their anode tends to suffer from particle cracking, loss of  $\text{Li}^+$  into the thickened SEI layer and poor contact between the anode and the other component of the cell as it shrinks upon cycling (Li et al., 2019). The net result of these degradations is an increase of interfacial impedances and failure of the cell.

In terms of new cathodes, LNMC 333 ( $\text{LiNi}_{0.33}\text{Co}_{0.33}\text{Mn}_{0.33}\text{O}_2$ ) coupled with Si/graphite is already commercialized (Dixit et al., 2017). However, their high capacity compromises their cyclability. Nickel rich NMC cathodes such as  $\text{LiNi}_{0.6}\text{Co}_{0.2}\text{Mn}_{0.2}\text{O}_2$  and  $\text{LiNi}_{0.8}\text{Co}_{0.1}\text{Mn}_{0.1}\text{O}_2$  tend to display poor cycling due to a gradual increase of higher oxidation states ions ( $\text{Ni}^{3+}$  and  $\text{Ni}^{4+}$

**TABLE 2** | Safety and capacity of the common anodic materials used in LiB. Reproduced with minor changes with permission from Goriparti et al. (2014).

Active anode material	Theoretical capacity (mAh g <sup>-1</sup> )	Advantages	Common issues
<b>INSERTION/DE-INSERTION MATERIALS</b>			
<b>A. Carbonaceous</b>			
a. Hard carbons	200–600	Good working potentials	Low coulombic efficiency
b. CNTS	1116	Low cost	High voltage hysteresis
c. Graphene*	780/1116	Good safety	High irreversible capacity
<b>B. Titanium oxides</b>			
a. LiTi <sub>4</sub> O <sub>5</sub>	175	Extreme safety	Very low capacity
b. TiO <sub>2</sub>	330	Good cycle life Low cost High power capability	Low energy density
<b>ALLOY/DE-ALLOY MATERIALS</b>			
a. Silicon	4212	High specific capacities	Large irreversible capacity
b. Germanium	1624	High energy density	Huge capacity fading
c. Tin	939	Good safety	Poor cycling
d. Antimony	660		
e. Tin oxide	790		
f. SiO	1600		
<b>CONVERSION MATERIALS</b>			
<b>Metal Oxides</b> (Fe <sub>2</sub> O <sub>3</sub> , Fe <sub>3</sub> O <sub>4</sub> , CoO, Co <sub>3</sub> O <sub>4</sub> , Mn <sub>x</sub> O <sub>y</sub> , Cu <sub>2</sub> O/CuO, NiO, Cr <sub>2</sub> O <sub>3</sub> , RuO <sub>2</sub> , MoO <sub>2</sub> /MoO <sub>3</sub> etc.)	500–1,200	High capacity High energy Low cost Environmentally compatibility	Low coulombic efficiency Unstable SEI formation Large potential hysteresis Poor cycle life
<b>B. Metal phosphides/sulfides/nitrides</b> (MX <sub>y</sub> ; M = Fe, Mn, Ni, Cu, Co etc. and X = P, S, N)	500–1800	High specific capacity Low operation potential and low polarization than counter oxides	poor capacity retention Short cycle life High cost of production

\*Significant interest in recent times due to high power density, long cycling life, and short charging time (Guo et al., 2017).



ions). Reactivity of these ions with electrolytes accelerate cathode degradation (Dixit et al., 2017).

Due to their high capacities and low cost rechargeable, lithium-sulfur batteries are the next most anticipated beyond Si/G||LNMC lithium ion cells (Ould Ely et al., 2018). Significant efforts are undertaken by the scientific community to pair the Li metal (3,860 mA h/g) anode, with high capacity sulfur

cathode (1,675 mAhg<sup>-1</sup>). This combination is expected to lead to a 500 Wh kg<sup>-1</sup> cell doubling the gravimetric energy of commercial Li ion batteries (~243 Wh kg<sup>-1</sup>) (Wei et al., 2015; Moreno et al., 2016). However, lithium metal anode needs to be shielded from conventional electrolytes and polysulfides shuttling.

Anodes based on lithium metal are still problematic due to lithium reactivity and propensity to deplete liquid electrolytes. Huang et al. (2014) reported a hybrid anode (graphite/lithium)

<sup>6</sup><https://www.bloomberg.com/graphics/2017-lithium-battery-future/>

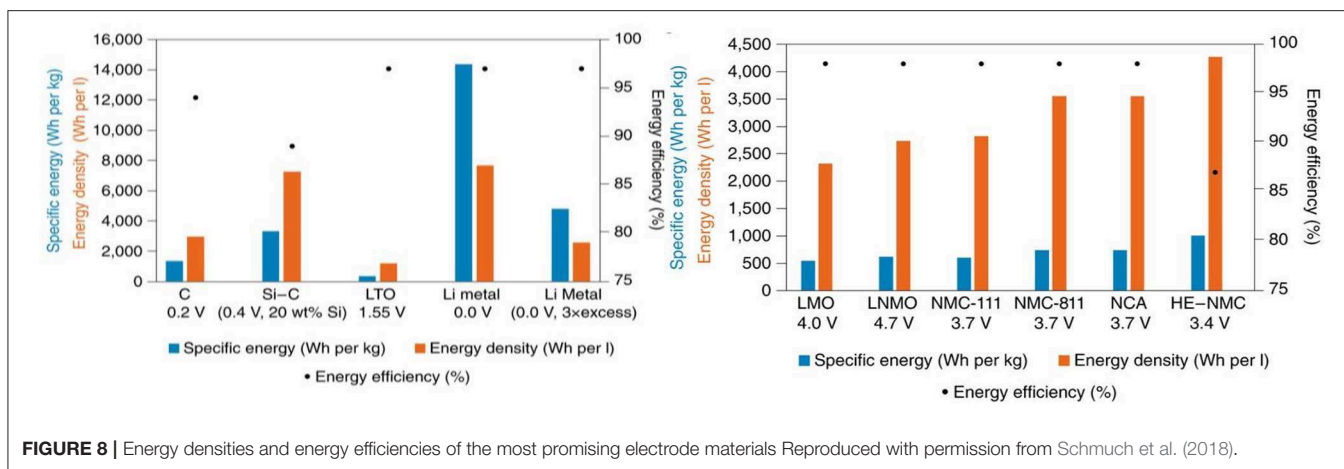


**FIGURE 8** | Energy densities and energy efficiencies of the most promising electrode materials Reproduced with permission from Schmuck et al. (2018).

that prevents electrolyte depletion and enables high capacity Li-S cell.

This cell is made by inserting a lithiated graphite layer between lithium metal and the electrolyte. In this hybrid anode, lithium metal serves as a reservoir for lithium ions and is completely shielded from direct contact with the electrolytes. Furthermore, the graphite layer limited the risk of dendritic growth and penetration and shielded lithium from reacting with the polysulfides.

This hybrid anodes enable Li-S to operate using conventional electrolyte at a capacity of more than  $800 \text{ mAh g}^{-1}$  for 400 cycles at a high rate of  $1,737 \text{ mA g}^{-1}$ , with excellent Coulombic efficiency  $>99\%$ . However, the risk of thermal runaway as a result of dendritic growth remains undefeated.

Solid-state electrolytes are viewed as an enabling technology for lithium metal based batteries, as they can suppress both flammable electrolytes and dendrites growth as we will discuss in the next section (Yang et al., 2017a).

## ELECTROLYTE SAFETY

### State of the Art

An electrolyte is a medium which consists of salts and solvents and enables ions transfer between a cathode and an anode. Progress in electrolyte safety is well-reviewed elsewhere (Kalhoff et al., 2015; Wang et al., 2019). We will restrict our review to the most promising electrolyte systems.

Electrolytic solutions can be divided into three categories: (1) aqueous, (2) nonaqueous (organic electrolytes), and (3) solid electrolytes. An ideal electrolyte should have high dielectric constant, low viscosity, high stability during the cell operation, low melting point, and high boiling point of electrolytic solutions, low cost, and high safety. However, it is impossible to find all these attributes in one single electrolyte.

Furthermore, electrolytes should be able to form stable SEI layers (Kalhoff et al., 2015). An SEI layer is a passivation layer that forms on the surface of the electrode and results from the interaction between the electrolyte and the active electrode materials. The SEI layer grows when the potential of either the anode or the cathode exceeds the boundary of the electrochemical

window of stability of the electrolytic solution. Electrolytes are expected to be stable when their lowest unoccupied molecular orbital (LUMO) is higher than the Fermi energy of the anode, otherwise, they will be reduced. Similarly, electrolytes are expected to be stable if their highest occupied molecular orbital (HOMO) is lower than the cathode's Fermi energy level. Most electrolytes tend to be particularly unstable at the anode side of the battery as their LUMO is higher than the reduction potentials of most common anodes (lithiated graphite ( $0.1 \text{ eV}$ ), Li metal ( $0 \text{ eV}$ )). The SEI layer in most organic electrolytes leads to an optimal thickness, porosity, and ion conductivity. In contrast, interfacing aqueous electrolytes with metallic anodes leads to a thick and irregular SEI layer that pulverizes upon cycling, leading to poor coulombic efficiency.

Recent research in the field of aqueous electrolytes led successfully to a series of high voltage and energy density cells (Suo et al., 2017; Wang et al., 2018). We will discuss these findings in more detail in the next section.

### Aqueous Electrolytes

In terms of safety, aqueous electrolytes are advantageous over organic electrolytes due to their availability, environmental friendliness, non-flammability, and low cost. However, their narrow electrochemical stability window and low energy density compared to conventional non-aqueous electrolytes are disadvantageous (Kim et al., 2014; Alias and Mohamad, 2015).

The electrochemical window of pure water is around  $1.23 \text{ V}$  ( $E^\circ_{\text{cell}} = E^\circ_{\text{cathode}} - E^\circ_{\text{anode}}$ ) at  $25^\circ\text{C}$  at pH 0 ( $[\text{H}^+] = 1.0 \text{ M}$ ). Depending on the pH, water dissociates within the operating voltage of LiB and forms hydrogen bubbles at the anode between  $2.21$  and  $3.04 \text{ V}$  vs. Li.

Suo et al. developed a *water in salt* concept that favored the formation of stable electrolyte-electrode interphase and expanded the window of aqueous batteries to  $\sim 3$  volts (Figures 9A,B). The cell obtained operates at  $2.3$  volts and cycles up to  $1,000$  times with  $100\%$  coulombic efficiency (Suo et al., 2015). Another milestone in aqueous Li-ion battery is reported recently (Yang et al., 2019) by the reversible Bromine/Chlorine conversion–intercalation chemistry in graphite (L-BCG) (Figure 9C). This approach led to a  $4.2 \text{ V}$

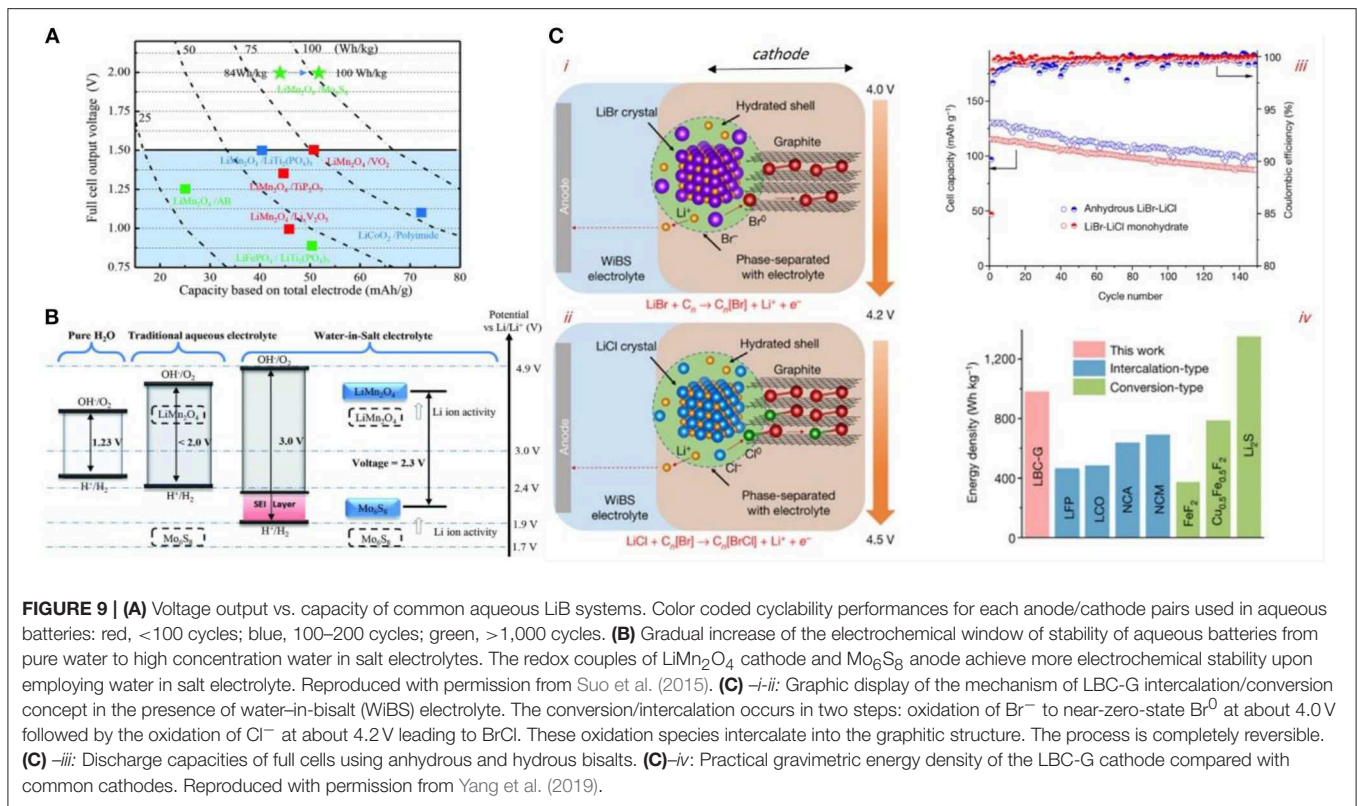


**TABLE 3 |** Thermodynamic characteristics of common solvents in which inorganic salts are dissolved to form organic electrolytes.

Electrolyte component	CAS registry number	molecular formula	Melting point	Boiling point	Vapor pressure (torr)	Flash point	Auto-ignition temperature	Heat of combustion
Propylene carbonate (PC)	108-32-7	$\text{C}_4\text{H}_6\text{O}_3$	$-49^\circ\text{C}$	$242^\circ\text{C}$	0.13 at $20^\circ\text{C}$	$135^\circ\text{C}$	$455^\circ\text{C}$	$-20.1 \text{ kJ/ml}$ $-4.8 \text{ kcal/ml}$
Ethylene carbonate (EC)	96-49-1	$\text{C}_3\text{H}_4\text{O}_3$	$36^\circ\text{C}$	$248^\circ\text{C}$	0.02 at $36^\circ\text{C}$	$145^\circ\text{C}$	$465^\circ\text{C}$	$-17.2 \text{ kJ/ml}$ $-4.1 \text{ kcal/ml}$
Di-methyl carbonate (DMC)	616-38-6	$\text{C}_3\text{H}_6\text{O}_3$	$2^\circ\text{C}$	$91^\circ\text{C}$	18 at $21^\circ\text{C}$	$18^\circ\text{C}$	$458^\circ\text{C}$	$-15.9 \text{ kJ/ml}$ $-3.8 \text{ kcal/ml}$
Diethyl carbonate (DEC)	105-58-8	$\text{C}_5\text{H}_{10}\text{O}_3$	$-43^\circ\text{C}$	$126^\circ\text{C}$	10 at $24^\circ\text{C}$	$25^\circ\text{C}$	$445^\circ\text{C}$	$-20.9 \text{ kJ/ml}$ $-5.0 \text{ kcal/ml}$
Ethyl methyl carbonate (EMC)	623-53-0	$\text{C}_4\text{H}_8\text{O}_3$	$-14^\circ\text{C}$	$107^\circ\text{C}$	27 at $25^\circ\text{C}$	$25^\circ\text{C}$	$440^\circ\text{C}$	None available

Reproduced with permission from Celina et al. (2011).

LiB aqueous cell with an estimated energy density of 460 Wh/kg and about 100% Coulombic efficiency. These discoveries may lead to aqueous batteries that are far safer than current state of the art of liquid batteries as reviewed elsewhere (Eftekhari, 2018).

Aqueous batteries still need further improvement in terms of expanding their potential window further and preventing the corrosion of their metallic current collectors (Church et al., 2014; Li and Church, 2017). Furthermore, long-term stability, shelf-life performances and scalability remain to be reported. The available current collectors on the market can be subjected to surface treatment to improve their resistance (Gheytni et al., 2016).

## Organic Electrolytes

Organic carbonates such as ethylene carbonate (EC) or diethyl carbonate (DEC) are the most common solvent used in organic electrolytes. This is primarily due to their high thermal stability,

electrochemical stability and ability to dissolve common inorganic salts such as  $\text{LiBF}_4$ ,  $\text{LiPF}_6$ ,  $\text{LiClO}_4$ , etc. (see Table 3).

$\text{LiPF}_6$  in particular is still one of the best salts in organic electrolytes on the market. However, this salt is thermally unstable and prone to hydrolysis (Celina et al., 2011).

The P-F bond in  $\text{LiPF}_6$  display strong reactivity toward hydrolysis. This reactivity can be minimized by substituting some of the fluorine atoms by bulky functional groups such as perfluorinated alkyl groups that can sterically shield phosphorus against hydrolysis (Ignat'ev et al., 2003).

In order to optimize the formation of SEI layer in organic electrolytes numerous alternative salts and additives have been investigated. Among these Lithium Difluoro bis(OxalatoBorate) ( $\text{LiFOB}$ ) salt which in spite of its lower conductivity favors a more sturdy and flexible SEI layer and reduces dendrite formation.  $\text{LiPF}_3(\text{C}_2\text{F}_5)_3$  ( $\text{LiFAP}$ ) is another salt that is more stable toward hydrolysis and less prone to flammability compared to  $\text{LiPF}_6$ .

Comparative studies of thermal stabilities of  $\text{LiPF}_6$  using accelerating rate calorimetry (ARC) shows its decomposition below  $200^\circ\text{C}$  while LiFAP degradation occurs above  $200^\circ\text{C}$  (Gnanaraj et al., 2003). Furthermore,  $\text{LiClO}_4$ ,  $\text{LiBF}_4$ ,  $\text{LiAsF}_6$ , and  $\text{LiSO}_3\text{CF}_3$  have been investigated as an electrolytic salt and are found to be less competitive with phosphorous based salts. For example,  $\text{LiClO}_4$  is super-reactive in contact with organics while  $\text{LiBF}_4$  tend to decompose at the anode side, in spite of being thermally stable and less prone to hydrolysis compared with  $\text{LiPF}_6$ . On the other hand,  $\text{LiAsF}_6$  is toxic, while solutions of  $\text{LiSO}_3\text{CF}_3$  have low conductivities.

### Ionic Liquids

Low melting points (usually, below  $100^\circ\text{C}$ ), non-flammable and thermally stable Ionic Liquids (ILs), are extensively investigated as potential replacement for organic electrolyte. These liquids have low vapor pressure, high specific conductivity, and wide electrochemical potential window of stability (up to 5.7 V) (Le Bideau et al., 2011; Wongitharom et al., 2013). These attributes are desirable for batteries safety (Roth and Orendorff, 2012).

Furthermore, some ionic liquids such as Butylmethylpyrrolidiniumbis(trifluoromethylsulfonyl)imide (BMP-TFSI) have high electrochemical stability, beyond Li plating reaction and are stable at high temperature and high potentials (Wongitharom et al., 2013) as confirmed by thermogravimetric analyses.

Similarly, piperidinium based ionic liquid electrolyte (Mun et al., 2010), in particular 1-allyl-1-methylpiperidinium bis(trifluoromethanesulfonyl)imide (AMPip-TFSI) displays high thermal stability than organic electrolytes (Mun et al., 2014).

One of the main disadvantage of ionic liquids is their high cost and high viscosity that ultimately lead to low conductivities. Mixing organic solvent with ionic liquid leads to electrolytes that retain safety properties of ILs and high conductivities of organic solutions. A content of more than 40% (IL:organic solvent) is found to improve thermal stability (Taggougui et al., 2008; Quinzeni et al., 2013).

Beside ionic liquids, an extensive list of flame retardant compounds such as alkyl phosphate, alkyl phosphonate (Yao et al., 2005; Zeng et al., 2014), and tetrabromobisphenol A (TBBA) are found (Nagasubramanian and Fenton, 2013) to improve the stability (Bae et al., 2013; Belov and Shieh, 2014) by scavenging and reacting with hydrogen radicals, thereby terminating the free radical reaction that leads to fire. Complete elimination of fire in Li-ion cells using ionic liquids and flame-retardant additives has yet to be achieved (Nagasubramanian and Fenton, 2013).

### Solid State Electrolytes

Due to their outstanding mechanical rigidity and ionic conductivities, lithium ion superconductor ceramics such as  $\text{Li}_7\text{La}_3\text{Zr}_2\text{O}_{12}$  (LLZO),  $\text{Li}_{1+x}\text{Al}_x\text{Ti}_{2-x}(\text{PO}_4)_3$  (LATP), and  $\text{Li}_2\text{S-P}_2\text{S}_5$  glasses (LPS), present the most promising and novel strategy to improve battery safety and suppress Li metal dendrite formation. However, numerous challenges need to be solved before an all solid-state battery can be commercialized. These challenges will be discussed in the next section.

## Novel Electrolytes and Future Challenges

Standard electrolytes are reactive with lithium, have low flash point of their solvents (FP) ( $<38.7^\circ\text{C}$ ) (Nagasubramanian and Fenton, 2013) and are prone to ignition and fire while ionic liquid and electrolytes with flame retardant additives have high viscosity and poor wettability. The development of a low-cost non-flammable electrolytes based on hydrofluoro electrolytes as co-solvent (Figure 10A) (Nagasubramanian and Fenton, 2013) greatly improved the safety and reliability of lithium ion batteries (Nagasubramanian and Orendorff, 2011). This is primarily due to their thermal stability and extremely high flash point. Furthermore, the recent development of a dual-electrolyte (or hybrid-electrolyte) opens new possibilities for mitigating dendrites' growth while maintaining the advantages of conventional organic liquid electrolytes (Wang et al., 2015). A dual-phase-non-aqueous electrolyte is composed of two types of electrolytes separated by lithium super ionic conductor membrane (LISICON) of  $\text{Li}_{1+x+y}\text{Al}_x\text{Ti}_{2-x}\text{Si}_y\text{P}_{3-y}\text{O}_{12}$  (LTAP) that transports lithium ion while blocking polysulfide-anions (Figure 10B).

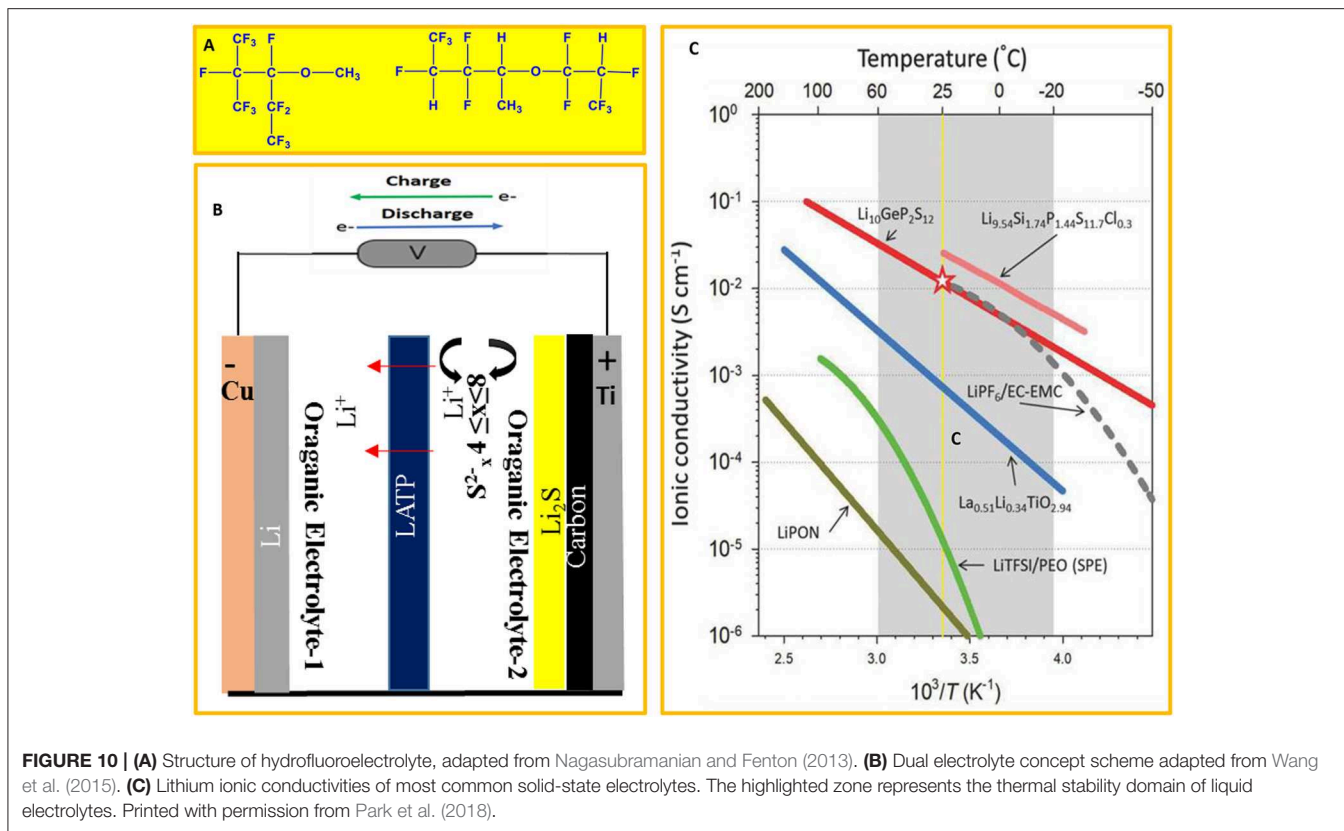
Solid-state electrolytes are viewed as the ultimate solution to eradicate both dendritic growth and polysulfides shuttling (Yang et al., 2017a). Solid state electrolytes and can be divided into two categories: inorganic solid electrolytes, and (2) organic solid polymer electrolytes.

In spite of their low cost, ease of processability organic solid polymer electrolytes have low room temperature conductivities and will not be reviewed here. On the other hand, inorganic solid-state electrolytes can be divided into two main categories: (1) sulfide solid state electrolytes and (2) oxide solid state electrolytes. Sulfide solid state electrolytes have high ionic conductivities comparable to liquid electrolyte at room temperature (Figure 10C). They can be cold pressed and yield good interfacial contact.

However, there are four requirements before an All-Solid-State Battery can be commercialized: (1) the reduction of interfacial impedances between these solid state ceramic and the electrode (both the anode and the cathode), (2) Reduction of the thickness and cost of the ion conducting ceramic separator ( $<100\ \mu\text{m}$  and cost no more than  $\$10/\text{m}^2$ ) (McCloskey, 2015). (3) Long-term cycle stability and high coulombic efficiency, (4) the stability of sulfide based  $\text{Li}^+$  conductors ceramic electrolyte in ambient atmosphere.

To achieve these requirements, various coating methods have been investigated to reduce interfacial impedances and suppress Li dendrite growth (Cheng et al., 2014; Zheng et al., 2014; Jing et al., 2015; Bucur et al., 2016; Zhu et al., 2017). Thin coating of the lithium anode by Li-Al alloy is found to improve the cycling performances by shielding lithium metal from polysulfides deposition, slowing down dendrites growth and reinforcing the SEI layer (Kim et al., 2013). The alloy layer must be in good contact with lithium metal to eliminate the interfacial resistances (Choudhury et al., 2017).

Using a trilayer Li-garnet-electrolyte architecture Hitz et al. (2019) developed an all-solid-state Li-S battery with an area specific resistances of  $\sim 7\ \Omega\text{cm}^2$ , and current densities higher ( $10\ \text{mA}/\text{cm}^2$ ). This promising work represents a first step toward safe full-scale solid-state batteries.



There are several strategies to optimize interfacial impedances of solid state electrolytes (Hood and Chi, 2019):

1. Domain structures optimization: in solid state electrolytes the SEI layer is primarily made of self-formed grain boundary interfacial domains with distinct phase structure and orientation. These domains are often characterized by high impedances and sluggish ion transport. Studies show that the smaller the size of these domains, the better the interfacial impedances. Furthermore, the domain sizes can be reduced by post annealing.
2. Composite interface optimization: organic/solid state ceramic interface has a conductivity that depends on each component. For example, the interface of PEO-LLZO display a barrier in front of lithium ion transport stronger than that of each component. In effect, lithium ion percolate either along PEO or LLZO, therefore by tuning the composite interface, the interface impedances can be optimized (Zheng et al., 2016).
3. Thermal treatment can reduce interfacial impedances as demonstrated by Sharafi et al. (2016) who demonstrated 10-fold decrease in interfacial resistance upon interfacial thermal treatment.
4. Insertion of a third conducting layer at the interface can reduce the resistance. This is commonly carried out by sputtering, passivation, or lithium wetting of a third layer at the interface between solid state electrolytes and electrode material.

## SEPARATOR DEGRADATION AND SAFETY

### Current State of the Art

Separators are one of the most effective safety measures against the internal short circuit. They are located between the positive electrode and the negative electrode to prevent electric short-circuiting and serve as an ion reservoir to enable free transport of lithium ions. Separators employed in Li-ion batteries are divided into two main classes: polymer based separators and ceramic based separators. Polymer-based separators are the most common separators and can be categorized into four main classes; microporous separators, non-woven mat separators, polymer electrolyte membranes, and composite membrane separators. Their characteristics and manufacturing are well-reviewed in recent literature (Zhang, 2007; Deimede and Elmasides, 2015; Jana et al., 2018). Typical parameters for LiB separators are summarized in **Table 4**.

Organic separators must be chemically inert, physically robust and satisfy all the requirement listed in **Table 4**.

### Polymer Based Separators

Due to their convenient chemical stability, mechanical strength and thickness, polymer separators based on polyolefin (mainly Polyethylene (PE) and Polypropylene (PP) are widely adopted in most commercial LiB (**Table 5**). They are used as single layer or multilayers. The multilayer separator are mechanically more robust and thermally

**TABLE 4** | General criteria for separators used in lithium-ion batteries.

Parameters	Requirement
Chemical and electrochemical stabilities	Stable in contact with the cell components for a long period of time
Wettability	Wet out quickly and completely
Mechanical property	$> 1,000 \text{ kg cm}^{-1}$ (98.06 MPa)
Thickness	20–25 micron
Pore size	$< 1$ micron
Porosity	40–60%
Permeability	$< 0.025 \text{ s/micron}$
Dimensional stability	No curl up and lay flat
Thermal stability	$< 5\%$ shrinkage after 60 min at 90
Shutdown	Effectively shut down the battery at elevated temp.

Reproduced with permission from Deimede and Elmasides (2015).

more stable than single layer separators. Trilayer ceramic separator displays the highest wettability, thermal stability and porosity among trilayer separators ( $> 220^\circ\text{C}$ , and porosity  $> 40$ ) (Abraham et al., 1995; Lee et al., 2005; Cho et al., 2007; Zhang, 2007; Ryou et al., 2011). Non-woven mats separators are by far the most promising separators due to their high porosity, small pore size, and large surface area. These attributes enable efficient wettability and good ionic conductivity although their mechanical robustness needs improvement.

Polymer separators typically have a porous structure, if the battery temperature increases to near the separator melting point, the separator pores will close and block the pathway between the positive and negative electrodes and terminate the electrochemical processes. This phenomenon is called “separator shutdown” and occurs around the melting point of the polymer separator;  $140^\circ\text{C}$  (for PE) and  $160^\circ\text{C}$  (for PP) (Kong et al., 2018a).

For high energy and power densities, separators should be very thin, have high wettability, high ionic conductivity, and high porosity. Furthermore, they should be mechanically robust and able to shut the battery down when overheating occurs to prevent thermal runaway. Properties of most common polymer separators are displayed on **Table 5**.

### Ceramic Based Separators

Next generation separator will inevitably have a composite structure to enable optimal thermal stability, mechanical strength, and conductivity. Ceramic coating of mono and multilayer separators increases mechanical resistance to thermal shrinkage and wettability (Roth et al., 2007; Shi et al., 2017). Alumina (Choi et al., 2010),  $\text{BaTiO}_3$  (Nunes-Pereira et al., 2014), and silicon oxides (Kang et al., 2012) among others have been reported. However, coating uniformity and processing should be controlled carefully to avoid defects during manufacturing and cell assembly. Defects in an  $\text{Al}_2\text{O}_3$  coated thin monolayer separator (1/5/1 microns:  $\text{Al}_2\text{O}_3/\text{polymer membrane}/\text{Al}_2\text{O}_3$ ) are among the factors behind thermal runaway and failure of Samsung Galaxy 7 in 2017 (Loveridge et al., 2018). Typical thickness for commercial separators is from 12 to  $25 \mu\text{m}$  (Orendorff, 2012).

**TABLE 5** | Commercial separators properties\* reproduced with permission from Orendorff (2012).

Product	Entek (Teklon)	Exxon (Tonen)	Degussa (separion)	Celgrad (2325)
Thickness ( $\mu\text{m}$ )	25	25	25	25
Single/multilayer	Single layer	Single layer	Trilayer	Trilayer
Composition	PE	PE	Ceramic-PET-Ceramic	PP-PE-PP
Process	Wet extruded	Wet extruded	Wait-laid mat	Dry extruded
Porosity (%)	38	36	$> 40$	41
Melt temperature	135	135	220	134/166

\*Separator specifications are found on data sheets for each product.

### Novel Separators Concept, Materials, and Chemistries

Next generation safe separators are expected to be fire resistant, have high mechanical strength, good thermomechanical stability, high ion-transport, and good wettability. However, achieving all these properties in one separator is a major challenge.

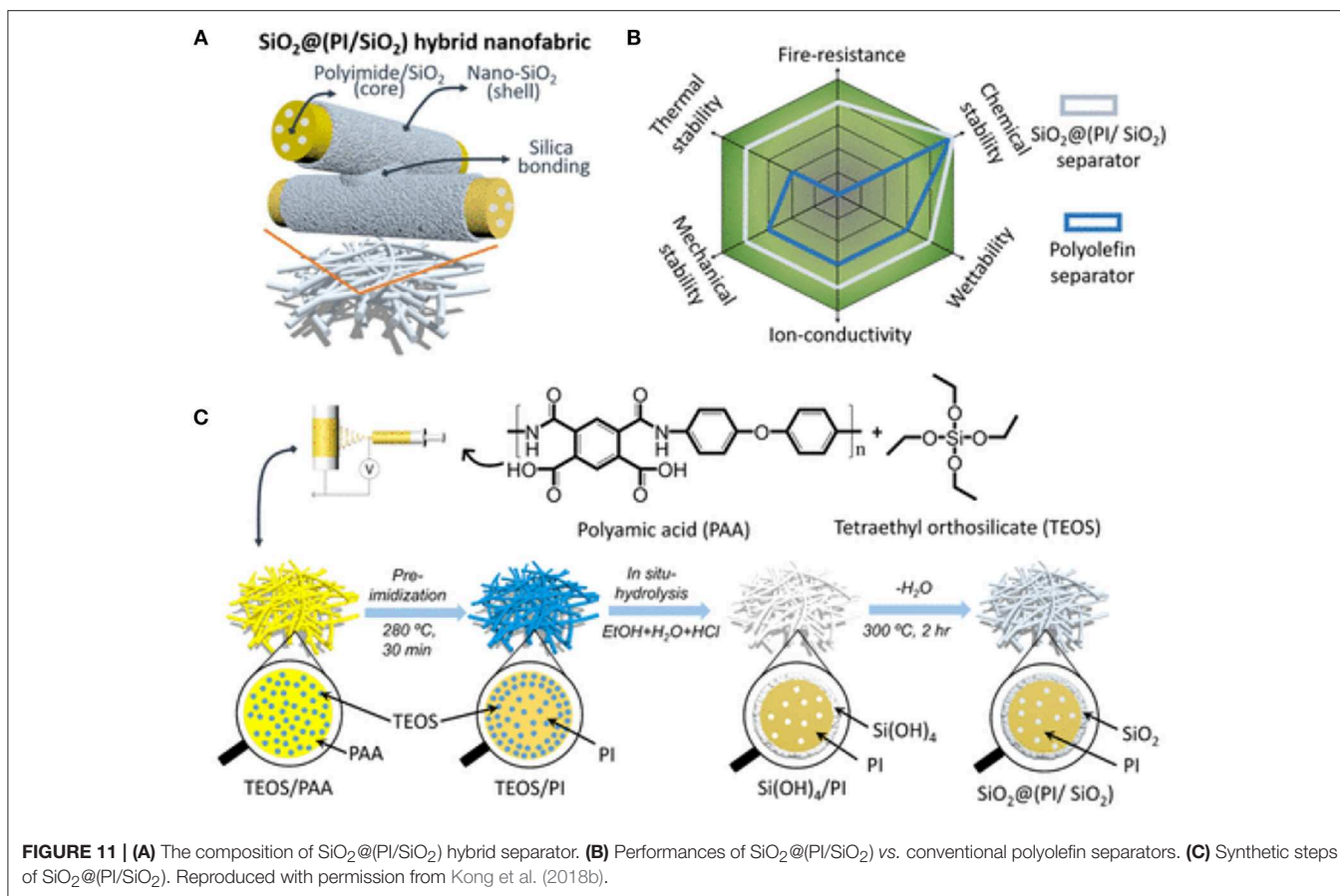
Polyimide (PI) nanofiber-based non-woven mats are among the safest separator materials reported so far. This is primarily due to their thermal stability up to  $500^\circ\text{C}$  whereas typical conventional polyolefin separators shrink at nearly  $150^\circ\text{C}$ . Moreover, PI nanofibers-based non-wovens have better electrolyte uptake of ions. A new hybrid PI based separator blended with nanostructured core-shell silica fillers  $\text{SiO}_2@(\text{PI}/\text{SiO}_2)$  is recently developed (see synthetic scheme in **Figure 11**) and showed high tensile strength, excellent wettability and good thermomechanical stability and fire resistance (Kong et al., 2018b).

A  $\text{LiFePO}_4$  half-cell assembled using  $\text{SiO}_2@(\text{PI}/\text{SiO}_2)$  hybrid separator displayed excellent rate capability at 5 C and high capacity of  $139 \text{ mAh}\cdot\text{g}^{-1}$ , compared to bare PI separator ( $126.2 \text{ mAh}\cdot\text{g}^{-1}$ ) and Celgard-2400 separator ( $95.1 \text{ mAh}\cdot\text{g}^{-1}$ ) (**Figure 12**). Furthermore, the half-cell showed an outstanding performance at high temperature ( $120^\circ\text{C}$ ) as confirmed by 100% columbic efficiency retention over 100 cycles.

Neither organic separators nor non-wovens nanofibers and PI based separators can detect and interdict the growth of dendrites. To achieve this objective, a new generation of smart separators that detect and interdict lithium dendrite growth is needed.

Wu et al. innovated a new type of bifunctional separators that detect the early growth of dendrites by monitoring voltage change on the walls of separator. This bifunctional separator can sense, predict and interdict thermal runaway (Wu et al., 2014). The bifunctional separator is prepared by stacking two conventional porous polymer separators and applying a copper layer onto one side of the polymer separator so that there is a third electrode between the cathode and anode. When the dendrite touches the copper layer of the separator, the voltage suddenly drops to zero and the battery may be disabled before the dendrite reaches the cathode (**Figure 13A**).

Ye et al. (2018) reported a smart separator composed of two conventional microporous polymer membranes sandwiching



a conducting graphene oxide layer (30  $\mu\text{m}$  thick). This trilayer separator efficiently prevented internal shorts upon subjecting the cell ( $\text{LMO}||\text{Polypropylene}/\text{GO}/\text{Polypropylene}||\text{Li}$ ) to intentional piercing. It is worth mentioning that the GO interlayer did not affect the battery capacity and rate capability performances as the cell can reversibly be charged/discharged for 6,000 cycles while retaining high coulombic efficiency of 93%. In the absence of this separator, the cell short-circuited after 125 cycles **Figure 13B**.

Furthermore, a novel self-extinguishing separator is synthesized by coating conventional PE separators with microcapsules filled with a fire-extinguishing agent (Yim et al., 2015). The fire extinguishing agent used is [1,1,1,2,2,3,4,5,5,5-decafluoro-3-methoxy-4-(trifluoromethyl)-pentane] (DMTP) with an endothermic enthalpy ( $\Delta H$ ) of  $+102.1 \text{ J g}^{-1}$ . The DMTP is encapsulated in a cross-linked PMMA shell to avoid any reactivity or contact with the electrolyte and its release is thermally triggered.

A DMTP loaded inside PMMA microcapsule coated on PE separator (mass loading of microcapsules =  $0.636 \text{ g g}^{-1}$  of PE) and blended with the electrolyte at 10 wt% ratio suppressed thermal runaway in a full-cell composed of  $\text{LiNi}_{0.5}\text{Co}_{0.2}\text{Mn}_{0.3}\text{O}_2$  cathode and a graphite anode. These microcapsules neither induced any capacity fading nor interfered with electrochemical performances of the cell.

## CURRENT COLLECTOR ROLE IN BATTERIES SAFETY

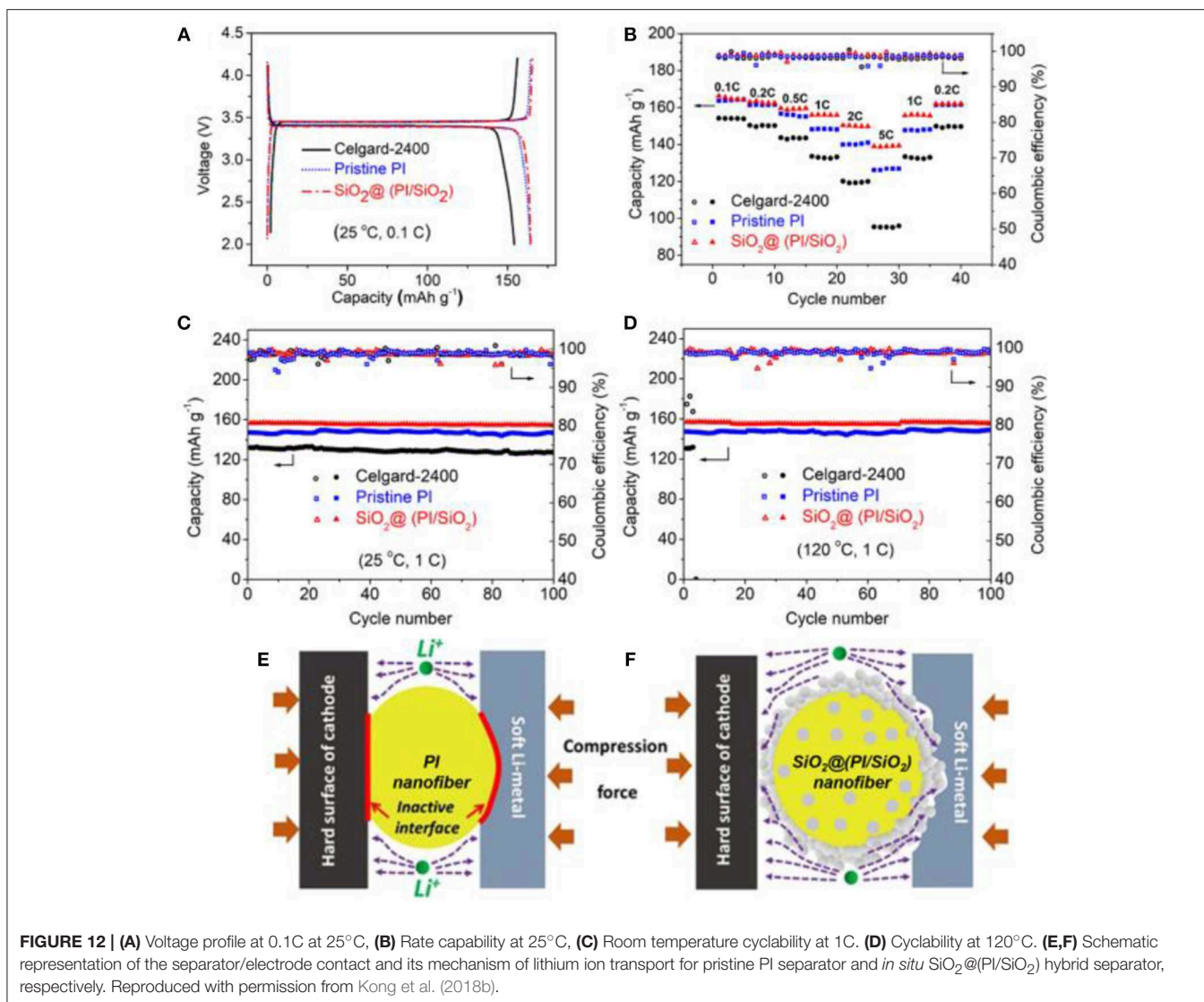
### State of the Art

The main safety hazard related to current collectors stems from their corrosion upon reacting with the electrolytes. It is crucial to select current collectors that are cheap, light weight, self-supporting, mechanically robust, and electrochemically inert within the voltage window of the battery. Current collectors of most commercial lithium ion batteries use copper for the anode side and aluminum for the cathode side.

Copper is selected due to its electrochemical stabilities at low potentials (0.01–0.25 V vs.  $\text{Li}/\text{Li}^+$  voltage), while aluminum has a reduction potential of 1.334 V vs.  $\text{Li}/\text{Li}^+$  and thus stable at high potentials. Nickel, brass, superalloys as well as nickel-aluminum superalloys are particularly promising due to their light weight, thermoresistive and anticorrosive properties (Bonnemann et al., 2002; Filippin et al., 2018).

### Novel Current Collector Concept, Materials, and Chemistries

Current collectors can be coated, patterned, or structured to suppress dendritic growth. Numerous approaches are investigated among these; nanowires based current collectors (Lu et al., 2016), 3D patterned current collectors (Umh et al.,



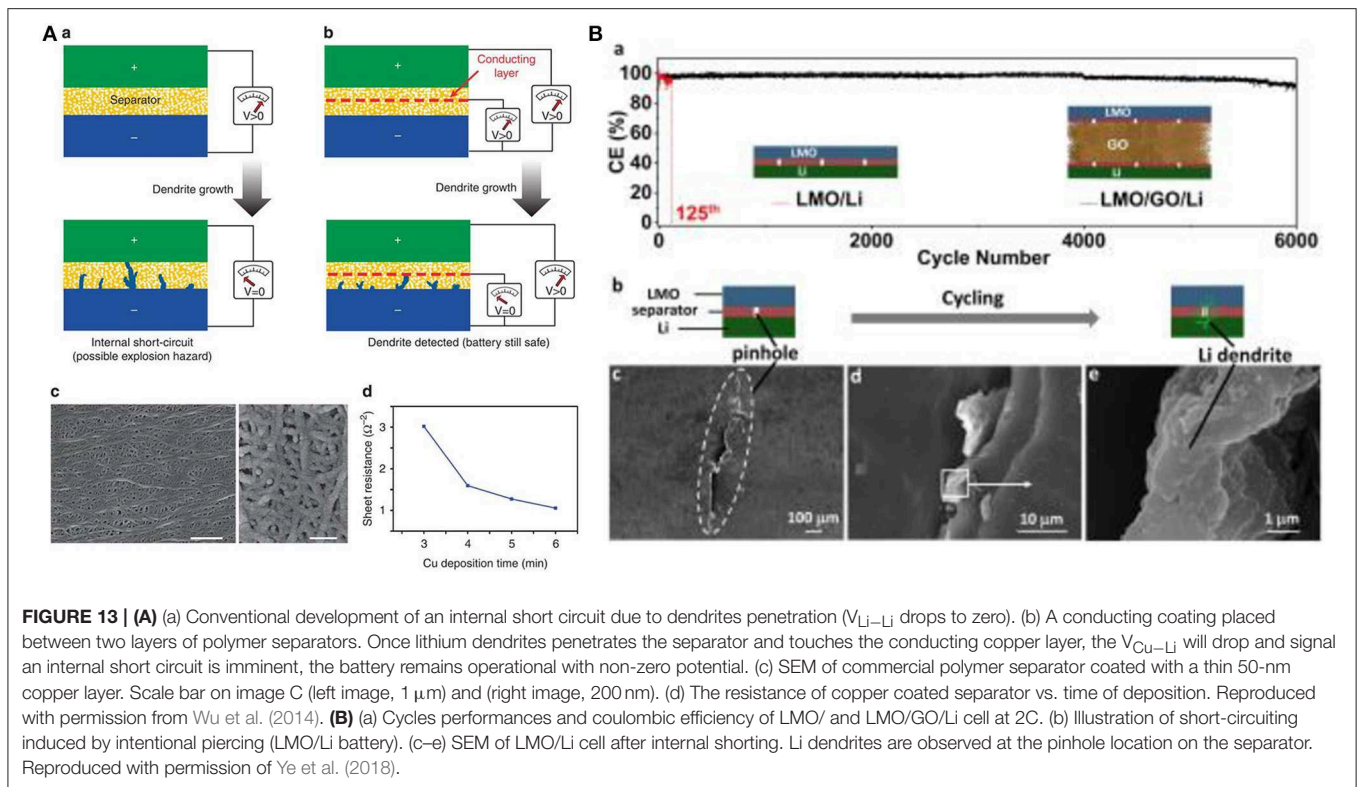
2019), foam-like current collectors (Mukanova et al., 2017, 2018; Lu et al., 2019), porous reduced graphene oxide/poly(acrylic acid) (rGO-PAA) aerogels based current collectors (Pender et al., 2019). These approaches revolve around the idea of changing the planar architecture of conventional current collectors to confine dendritic growth or redirect it away from the separator. We will discuss the most successful strategies to suppress dendritic growth using architected current collectors. These strategies can be grouped into three classes: (1) Control of nucleation over-potential. (2) Redirection of dendritic growth, (3) Containment of dendritic growth.

- **Control of lithium nucleation over-potential:** this concept relies on providing a large number of nucleation sites to prevent dendritic growth from penetrating separators (Yang et al., 2017b; Yue and Liang, 2018; Zhang C. et al., 2018; Huang et al., 2019; Umh et al., 2019). For example, a novel current collector made of carbon nitride coated on 3D Ni foam ( $g\text{-C}_3\text{N}_4\text{/Ni}$  foam) led to dendrite-free Li metal cells with CE of 98%

after 300 cycles (Lu et al., 2019). The suppression of dendritic growth is due to the presence of large number of microelectric field and nucleation sites available for lithium nucleation. Lithiophilic coating of these nickel foam with graphitic carbon nitride  $g\text{-C}_3\text{N}_4$  leads to low Li nucleation overpotential that suppresses dendritic growth (Lu et al., 2019).

The advantage of structured current collectors is overshadowed by their expensive synthesis and inconvenient large surface area that usually produces high electrode/electrolyte interface area and causes significant consumption of electrolyte and Li species and consequently low Coulombic efficiency due to an excessive growth of SEI layer.

- **Dendritic growth diversion:** the idea here is to provide a superstructure network that confines lithium dendrites growth within the current collector rather than toward the separator. For example; macroporous dendritic copper current collector was found to decrease the ion flux density



and enhance the homogeneity of Li-ion flux distribution providing homogenous growth that precludes the formation of dendrites. This current collector outperforms conventional planar copper current collectors in terms of coulombic efficiency, as can be seen on the **Figure 14A**.

- **Dendritic growth containment:** this concept relies on containing dendritic growth in a special compartment of the current collector, enabling the battery to operate in spite of the presence of dendritic lithium. The electric field in this type of current collectors is localized laterally and thus guides dendritic growth laterally within the interior of the copper scaffold compartment. This compartmented current collector (**Figures 14Ba–c,C**) was tested in full cell against  $\text{LiFePO}_4$  as a cathode. The cell  $\text{Cu@Li//LiFePO}_4$  was cycled for 250 cycles at 1 C rate and showed remarkable coulombic efficiency compared to the planar copper current collector (**Figure 14C**).

Finally, dendritic growth can be affected by pressure. Recent theoretical calculations provide a predictive model for dendritic growth and protrusion suppression based on the impact of external pressure and electrolyte transport properties. It was observed that large magnitudes of externally applied pressure cause plastic deformation of lithium metal, which helps in preventing the growth of dendritic protrusions (Barai et al., 2018).

## CONCLUSION AND FUTURE OUTLOOK

Battery manufacturers and governments around the world are seeking ways to reduce greenhouse gases by integrating

high capacity batteries into public transportation and storing renewable energies for intermittent use.

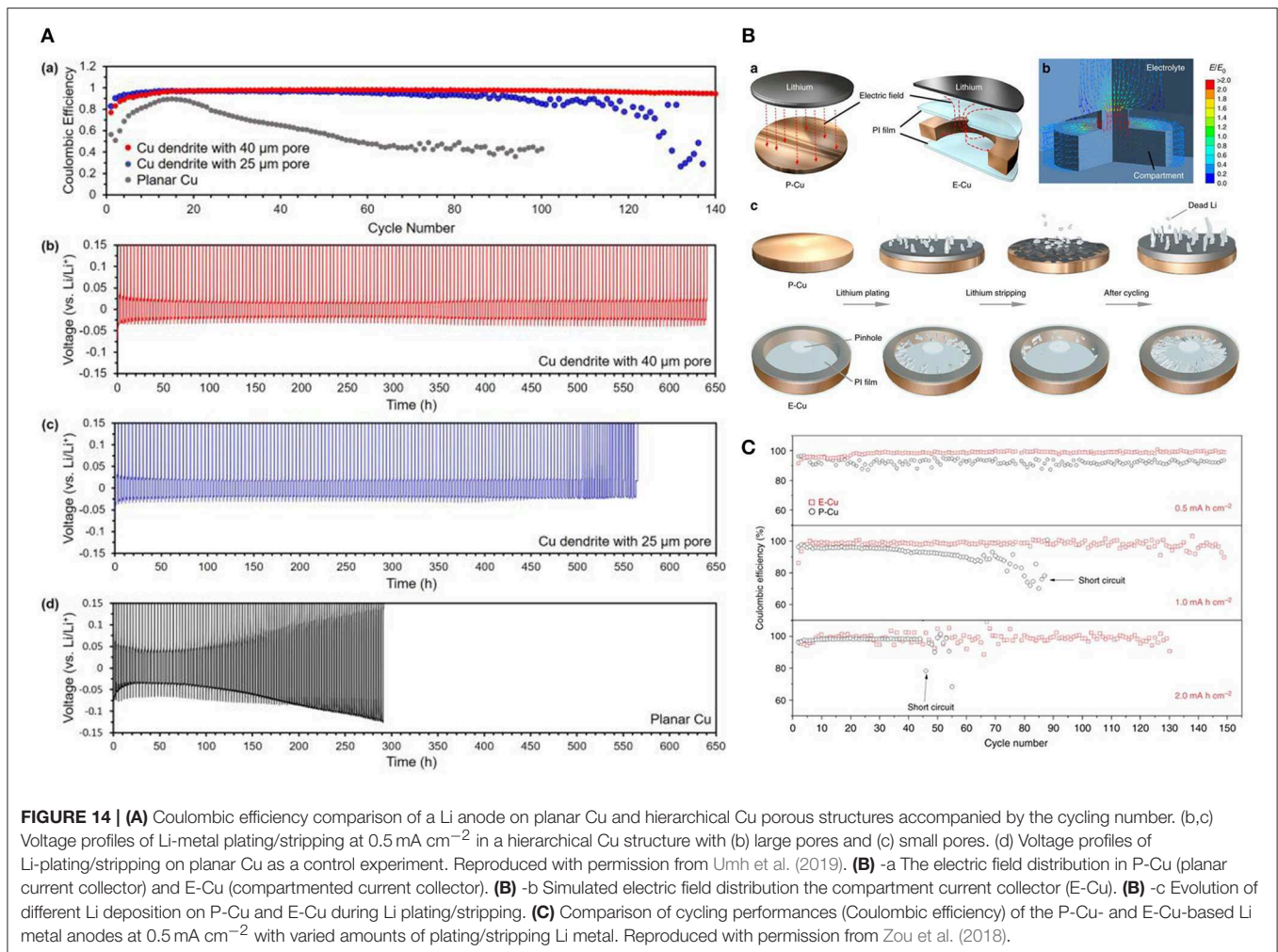
Due to their high power and high capacity characteristics, LiB are relevant to many applications and are expected, as we highlighted in this review, to continue improving in all their aspects (improved electrode materials, robust separators, non-flammable electrolytes, structured current collectors, improved cell and multicell pack design).

As we have seen throughout this review, the safety features currently employed are either too expensive which preclude their commercialization or ineffective in predicting and eliminating internally triggered thermal runaway.

The complexity arises from the fact that lithium dendrites growth can originate from many interrelated factors that act separately or simultaneously to trigger thermal runaway. Nevertheless, thermal runaway occurrence is rare but can cause huge financial loss. The recall of Samsung Galaxy 7 in 2017, led to an estimated loss of 17 billion USD, while the grounding of the Boeing 787 Dreamliner in 2013 due to lithium ion battery problems costed the company and estimated loss of 1.1 million USD a day.

The growth of lithium dendrites is one of the main trigger of thermal runaway and has been mitigated by four main approaches: (1) *capping* using either additive molecules or ions, (2) *redirection* of dendritic growth away from separators using lithiophilic/lithiophobic coating, (3) *containment* in a compartment/structured current collector, (4) suppression using solid state electrolyte.

Beside dendrites elimination, minimization of exothermic redox reactions between the anode, and the cathode should



be taken into consideration upon designing safer batteries. Comprehensive thermal analysis showed that heat generated during thermal runaway mostly comes from these redox reactions (Feng et al., 2019).

Recent progress in solid state electrolytes is the most promising technology to provide radical solution to thermal runaway and enable batteries beyond current lithium ion. In an all-solid state-battery the active components that are prone to degradation upon aging can be limited to both electrodes since it excludes the use of binders, separators, and liquid electrolytes, thus reduce the risk of thermal runaway considerably. Furthermore, controlling dendritic growth of lithium is easier in an all-solid-state battery compared to liquid batteries since it depends primarily on our ability to master structural defects (crack along the grain boundaries and stacking faults among others). These defects originate from materials synthesis and processing and create high local current densities that promote an uneven lithium plating. The recent use of high temperature superalloys that have limited stacking fault and surface defects as current collectors combined with 3D lithiophilic nano-coating may reduce further the risk of dendritic growth in an all solid-state batteries.

For future commercialization of an all solid-state battery the scientific community still needs to address the four following requirements:

- (1) The reduction of interfacial impedances between solid state ceramic electrolyte and the electrode (both the anode and especially the cathode) to an area specific resistance (ASR)  $< 25 \text{ } \Omega\text{-cm}^2$  (currently total cell resistance of commercial Li-ion battery is  $\sim 22 \text{ } \Omega\text{-cm}^2$  for the liquid cells). Most solid-state ceramic electrolytes have an ASR for ceramic-Li metal interfaces ranging from 37 to  $\sim 20,000 \text{ } \Omega\text{-cm}^2$ . The cathode is even higher. The recent work on trilayer Li-garnet-electrolyte architecture by Hitz et al. (2019) led to low interfacial impedances ( $\sim 7 \text{ } \Omega\text{cm}^2$ ) and high current densities ( $10 \text{ mA/cm}^2$ ). However, the cost of manufacturing remain to be compared with current state of the art.
- (2) Reduction of the thickness and cost of the ion conducting ceramic separator ( $< 40\text{--}100 \text{ } \mu\text{m}$  and cost no more than  $\$10/\text{m}^2$ ) (McCloskey, 2015).
- (3) Long-term cycle stability and high coulombic efficiency.
- (4) The stability of sulfide-based  $\text{Li}^+$  conductors ceramic electrolyte in ambient atmosphere.

We are optimistic that most of these requirements will be met in the next few years. The advance of computational predictive model for materials selection coupled with density functional theory molecular dynamics (DFT-MD) calculations will provide precise identification of the next most promising class of superionic Li ion conductors ( $\geq 10^{-4}$  S/cm) at room temperature. Materials Synthetic Chemists will have the task to synthesize and scale up these materials. A number of promising candidates have already been identified by machine learning computational methods among these;  $\text{Li}_5\text{B}_7\text{S}_{13}$ ,  $\text{Li}_2\text{B}_2\text{S}_5$ ,  $\text{Li}_3\text{ErCl}_6$ ,  $\text{LiSO}_3\text{F}$ ,  $\text{Li}_3\text{InCl}_6$ ,  $\text{Li}_2\text{HfO}$ ,  $\text{LiMgB}_3(\text{H}_9\text{N})_2$ , and  $\text{CsLi}_2\text{BS}_3$ . Based on DFT-MD  $\text{Li}_5\text{B}_7\text{S}_{13}$ , is predicted to have a Li conductivity (74 mS/cm) many times larger than the fastest known Li ion conductors today (Sendek et al., 2018).

Furthermore, advances in big data and machine learning combined with remote battery management systems (BMS)

need further attention as it may help in mapping out the conditions that are likely to trigger thermal runaway events. This alongside with advances in new safe materials and chemistries (Yang et al., 2019) will enable safer batteries and accelerate large scale adoption of LiB and batteries beyond lithium ion in public transportation and other technological sectors.

## AUTHOR CONTRIBUTIONS

All authors listed have made a substantial, direct and intellectual contribution to the work, and approved it for publication.

## ACKNOWLEDGMENTS

TO would like thank Prof. Mike F. Doherty and the UCSB Chemical Engineering Department for hosting.

## REFERENCES

- Abraham, K. M., Alamgir, M., and Hoffman, D. K. (1995). Polymer electrolytes reinforced by Celgard membranes. *J. Electrochem. Soc.* 142, 683–7. doi: 10.1149/1.2048517
- Alias, N., and Mohamad, A. A. (2015). Advances of aqueous rechargeable lithium-ion battery: a review. *J. Power Sources* 274, 237–251. doi: 10.1016/j.jpowsour.2014.10.009
- Amine, K., Belharouak, I., Chen, Z., Tran, T., Yumoto, H., Ota, N., et al. (2010). Nanostructured anode material for high-power battery system in electric vehicles. *Adv. Mater.* 22, 3052–3057. doi: 10.1002/adma.201000441
- Armand, M. (1980). “Intercalation electrodes,” in *Materials for Advanced Batteries*, eds D. W. Murphy, J. Broadhead, and B. C. H. Steele (New York, NY: Plenum Press) 145. doi: 10.1007/978-1-4684-3851-2\_7
- Aurbach, D., Zinigrad, E., Teller, H., and Dan, P. (2000). Factors which limit the cycle life of rechargeable lithium (metal) batteries. *J. Electrochem. Soc.* 147, 1274–1279. doi: 10.1149/1.1393349
- Bae, S. Y., Shim, E. G., and Kim, D. W. (2013). Effect of ionic liquid as a flame-retarding additive on the cycling performance and thermal stability of lithium-ion batteries. *J. Power Sources* 244, 266–271. doi: 10.1016/j.jpowsour.2013.01.100
- Bai, P., Guo, J., Wang, M., Kushima, A., Su, L., Li, J., et al. (2018). Interactions between lithium growths and nanoporous ceramic separators. *Joule* 2, 2434–2449. doi: 10.1016/j.joule.2018.08.018
- Barai, P., Higa, K., and Srinivasan, V. (2018). Impact of external pressure and electrolyte transport properties on lithium dendrite growth. *J. Electrochem. Soc.* 165, A2654–A2666. doi: 10.1149/2.0651811jes
- Belov, D. G., and Shieh, D. (2014). A study of tetrabromobisphenol A (TBBA) as a flame retardant additive for Li-ion battery electrolytes. *J. Power Sources* 247, 865–875. doi: 10.1016/j.jpowsour.2013.08.143
- Besenhard, J. O., and Eichinger, G. (1976). High energy density lithium cells. Part I. Electrolytes and anodes. *J. Electroanal. Chem. Interfacial Electrochem.* 68, 1–18. doi: 10.1016/S0022-0728(76)80298-7
- Beyerle, R. A. II., McCallum, I. A., Smalc, M. D., Taylor, J. A., and Wayne, R. J. (2013). *Battery Pack Assembly with Thermal Management Structures*. US Patent No. 20130323564 A1 20131205. U.S. Patent Application Public.
- Bonnemann, H., Brijoux, W., Hofstadt, H.-W., Ould-Ely, T., Schmidt, W., Wassmuth, B., et al. (2002). Wet chemistry synthesis of  $\beta$ -nickel aluminide NiAl. *Angew. Chem. Int. Ed.* 41, 599–603. doi: 10.1002/1521-3773(20020215)41:4<599::AID-ANIE599>3.0.CO;2-R
- Bucur, C. B., Lita, A., Osada, N., and Muldoon, J. (2016). A soft, multilayered lithium-electrolyte interface. *Energy Environ. Sci.* 9, 112–116. doi: 10.1039/C5EE03056K
- Celina, M., Michael, K., Kevin, W., and Richard, T. L. (2011). *Lithium-Ion Batteries Hazard and Use Assessment Batteries Failure Analysis*. Exponent. Available online at: <https://www.nrc.gov/docs/ML1719/ML17191A294.pdf> (accessed July, 2019).
- Cheng, X.-B., Peng, H.-J., Huang, J.-Q., Wei, F., and Zhang, Q. (2014). Dendrite-free nanostructured anode: entrapment of lithium in a 3D fibrous matrix for ultra-stable lithium-sulfur batteries. *Small* 10, 4257–4263. doi: 10.1002/smll.201470130
- Chi, S.-S., Liu, Y., Song, W.-L., Fan, L.-Z., and Zhang, Q. (2017). Pre-storing lithium into stable 3D nickel foam host as dendrite-free lithium metal anode. *Adv. Funct. Mater.* 27:1700348. doi: 10.1002/adfm.201770151
- Cho, T. H., Sakai, T., Tanase, S., Kimura, K., Kondo, Y., Tarao, T., et al. (2007). Electrochemical performances of polyacrylonitrile nanofiber-based nonwoven separator for lithium-ion battery. *Electrochem. Solid State Lett.* 10, A159–A162. doi: 10.1149/1.2730727
- Choi, J.-A., Kim, S. H., and Kim, D.-W. (2010). Enhancement of thermal stability and cycling performance in lithium-ion cells through the use of ceramic-coated separators. *J. Power Sources* 195, 6192–6196. doi: 10.1016/j.jpowsour.2009.11.020
- Choudhury, S., Tu, Z., Stalin, S., Vu, D., Fawole, K., Gunceler, D., et al. (2017). Electroless formation of hybrid lithium anodes for fast interfacial ion transport. *Angew. Chem. Int. Ed.* 56, 13070–13077. doi: 10.1002/anie.201707754
- Church, B. C., Kaminski, D. T., and Jiang, J. (2014). Corrosion of aluminum electrodes in aqueous slurries for lithium-ion batteries. *J. Mater. Sci.* 49, 3234–3241. doi: 10.1007/s10853-014-8028-3
- Deimede, V., and Elmasides, C. (2015). Separators for lithium-ion batteries: a review on the production processes and recent developments. *Energy Technol.* 3, 453–468. doi: 10.1002/ente.201402215
- Deng, Y., Yang, C., Zou, K., Qin, X., Zhao, Z., and Chen, G. (2017). Recent advances of Mn-Rich LiFe<sub>1-y</sub>Mn<sub>y</sub>PO<sub>4</sub> (0.5  $\leq$  y < 1.0) cathode materials for high energy density lithium ion batteries. *Adv. Energy Mater.* 7:1601958. doi: 10.1002/aenm.201601958
- Ding, F., Xu, W., Graff, G. L., Zhang, J., Sushko, M. L., Chen, X., et al. (2013). Dendrite-free lithium deposition via self-healing electrostatic shield mechanism. *J. Am. Chem. Soc.* 135, 4450–4456. doi: 10.1021/ja312241y
- Dixit, M., Markovsky, B., Schipper, F., Aurbach, D., and Major, D. T. (2017). Origin of structural degradation during cycling and low thermal stability of ni-rich layered transition metal-based electrode materials. *J. Phys. Chem. C* 121, 22628–22636. doi: 10.1021/acs.jpcc.7b06122
- Doughty, D., and Roth, E. P. (2012). A general discussion of lithium ion batteries. *Electrochem. Soc. Interface Summer* 21, 37–44. doi: 10.1149/2.F03122if
- Eftekhari, A. (2018). High-energy aqueous lithium batteries. *Adv. Energy Mater.* 8:1801156. doi: 10.1002/aenm.201801156

- Eichinger, G., and Besenhard, J. O. (1976). High energy density lithium cells. Part II. Cathodes and complete cells. *J. Electroanal. Chem. Interfacial Electrochem.* 72, 1–31. doi: 10.1016/S0022-0728(76)80072-1
- FAA Office of Security and Hazardous Materials B. B.-P. D (1991). *Aviation Incidents; Involving Smoke, F., Extreme Heat or Explosion, incidents recorded as of March 20, 1991*. Available online at: [https://www.faa.gov/hazmat/resources/lithium\\_batteries/media/Battery\\_incident\\_chart.pdf](https://www.faa.gov/hazmat/resources/lithium_batteries/media/Battery_incident_chart.pdf)
- Feng, X., Sun, J., Ouyang, M., Wang, F., He, X., Lu, L., et al. (2015). Characterization of penetration induced thermal runaway propagation process within a large format lithium ion battery module. *J. Power Sources* 275, 261–273. doi: 10.1016/j.jpowsour.2014.11.017
- Feng, X., Zheng, S., Ren, D., He, X., Wang, L., Cui, H., et al. (2019). Investigating the thermal runaway mechanisms of lithium-ion batteries based on thermal analysis database. *Appl. Energy* 246, 53–64. doi: 10.1016/j.apenergy.2019.04.009
- Feng, X. O. M., Liu, X., Lu, L., Xia, Y., and He, X. (2018). Thermal runaway mechanism of lithium ion battery for electric vehicles: a review. *Energy Storage Mater.* 10, 246–267. doi: 10.1016/j.ensm.2017.05.013
- Filippin, A. N., Lin, T.-Y., Rawlence, M., Zund, T., Kravchyk, K., Sastre-Pellicer, J., et al. (2018). Ni-Al-Cr superalloy as high temperature cathode current collector for advanced thin film Li batteries. *RSC Adv.* 8, 20304–20313. doi: 10.1039/C8RA02461H
- Finegan, D. P., Darcy, E., Keyser, M., Tjaden, B., Heenan, T. M. M., Jervis, R., et al. (2018). Identifying the cause of rupture of Li-Ion batteries during thermal runaway. *Adv. Sci.* 5:1700369. doi: 10.1002/adv.201700369
- Finegan, D. P., Scheel, M., Robinson, J. B., Tjaden, B., Hunt, I., Mason, T. J., et al. (2015). In-operando high-speed tomography of lithium-ion batteries during thermal runaway. *Nat. Commun.* 6:6924. doi: 10.1038/ncomms7924
- Gheyfani, S., Liang, Y., Jing, Y., Xu, J. Q., and Yao, Y. (2016). Chromate conversion coated aluminium as a light-weight and corrosion-resistant current collector for aqueous lithium-ion batteries. *J. Mater. Chem. A Mater. Energy Sust.* 4, 395–399. doi: 10.1039/C5TA007366A
- Gnanaraj, J. S., Zinigrad, E., Asraf, L., Sprecher, M., Gottlieb, H. E., Geissler, W., et al. (2003). On the use of LiPF<sub>3</sub>(CF<sub>2</sub>CF<sub>3</sub>)<sub>3</sub> (LiFAP) solutions for Li-ion batteries. Electrochemical and thermal studies. *Electrochem. Commun.* 5, 946–951. doi: 10.1016/j.elecom.2003.08.020
- Goriparti, S., Miele, E., De Angelis, F., Di Fabrizio, E., Proietti Zaccaria, R., and Capiglia, C. (2014). Review on recent progress of nanostructured anode materials for Li-ion batteries. *J. Power Sources* 257, 421–443. doi: 10.1016/j.jpowsour.2013.11.103
- Graetz, J., Ahn, C. C., Yazami, R., and Fultz, B. (2004). Nanocrystalline and thin film germanium electrodes with high lithium capacity and high rate capabilities. *J. Electrochem. Soc.* 151, A698–A702. doi: 10.1149/1.1697412
- Guo, X., Zheng, S., Zhang, G., Xiao, X., Li, X., Xu, Y., et al. (2017). Nanostructured graphene-based materials for flexible energy storage, Energy storage materials. *Energy Storage Mater.* 9, 150–169. doi: 10.1016/j.ensm.2017.07.006
- Hauwiller, M. R., Zhang, X., Liang, W.-I., Chiu, C.-H., Zhang, Q., Zheng, W., et al. (2018). Dynamics of nanoscale dendrite formation in solution growth revealed through *in situ* liquid cell electron microscopy. *Nano Lett.* 18, 6427–6433. doi: 10.1021/acs.nanolett.8b02819
- Herold, A. (1955). Insertion compounds of graphite with bromine and the alkali metals. *Bull. Soc. Chim. Fr.* 187, 999–1012.
- Hitz, G. T., McOwen, D. W., Zhang, L., Ma, Z., Fu, Z., Wen, Y., et al. (2019). High-rate lithium cycling in a scalable trilayer Li-garnet-electrolyte architecture. *Mater. Today* 22, 50–57. doi: 10.1016/j.mattod.2018.04.004
- Hood, Z. D., and Chi, M. (2019). Mechanistic understanding and strategies to design interfaces of solid electrolytes: insights gained from transmission electron microscopy. *J. Mater. Sci.* 54, 10571–10594. doi: 10.1007/s10853-019-03633-2
- Hu, Z., Zhang, S., Zhang, C., and Cui, G. (2016). High performance germanium-based anode materials. *Coord. Chem. Rev.* 326, 34–85. doi: 10.1016/j.ccr.2016.08.002
- Huang, C., Xiao, J., Shao, Y., Zheng, J., Bennett, W. D., Lu, D., et al. (2014). Manipulating surface reactions in lithium-sulfur batteries using hybrid anode structures. *Nat. Commun.* 5, 4015/1–4015/7. doi: 10.1038/ncomms4343
- Huang, S., Tang, L., Najafabadi, H. S., Chen, S., and Ren, Z. (2017). A highly flexible semi-tubular carbon film for stable lithium metal anodes in high-performance batteries. *Nano Energy* 38, 504–509. doi: 10.1016/j.nanoen.2017.06.030
- Huang, S., Zhang, W., Ming, H., Cao, G., Fan, L.-Z., and Zhang, H. (2019). Chemical energy release driven lithiophilic layer on 1 m2 commercial brass mesh toward highly stable lithium metal batteries. *Nano Lett.* 19, 1832–1837. doi: 10.1021/acs.nanolett.8b04919
- Hunter, J. C. (1981). Preparation of a new crystal form of manganese dioxide:  $\lambda$ -MnO<sub>2</sub>. *J. Solid State Chem.* 39, 142–7. doi: 10.1016/0022-4596(81)90323-6
- Ignat'ev, N. V., Schmidt, M., Kuehner, A., Heider, U., Hilarius, V., Oesten, R., et al. (2003). "Synthesis of new Li-fluoroalkyl phosphates (LiFAPs) for application in Li-cells," in *Proceedings - Electrochemical Society. 2001-21 (Batteries and Supercapacitors)* (Germany: Merck KGaA /Darmstadt), 395–399.
- Jana, K. K., Lue, S. J., Huang, A., Soesanto, J. F., and Tung, K.-L. (2018). Separator membranes for high energy-density batteries. *ChemBioEng Rev.* 5, 346–371. doi: 10.1002/cben.201800014
- Jing, H.-K., Kong, L.-L., Liu, S., Li, G.-R., and Gao, X.-P. (2015). Protected lithium anode with porous Al<sub>2</sub>O<sub>3</sub> layer for lithium-sulfur battery. *J. Mater. Chem. A Mater. Energy Sust.* 3, 12213–12219. doi: 10.1039/C5TA01490E
- Julien, C., Mauger, A., Vjih, A., and Zaghbi, K. (2016). *Lithium Batteries Science and Technology*. Switzerland: Springer International Publishing.
- Juza, R., and Wehle, V. (1965). Lithium-graphite clathrates. *Naturwissenschaften* 52:560. doi: 10.1007/BF00631568
- Kalhoff, J., Eshetu, G. G., Bresser, D., and Passerini, S. (2015). Safer electrolytes for lithium-ion batteries: state of the art and perspectives. *ChemSusChem* 8, 2154–2175. doi: 10.1002/cssc.201500284
- Kang, S. M., Ryou, M.-H., Choi, J. W., and Lee, H. (2012). Mussel- and diatom-inspired silica coating on separators yields improved power and safety in Li-Ion batteries. *Chem. Mater.* 24, 3481–3485. doi: 10.1021/cm301967f
- Kelly, A. T., Rusakova, I., Ould-Ely, T., Hofmann, C., Luettge, A., and Whitmire, K. H. (2007). Iron phosphide nanostructures produced from a single-source organometallic precursor: nanorods, bundles, crosses, and spherulites. *Nano Lett.* 7, 2920–2925. doi: 10.1021/nl0713225
- Kim, H., Hong, J., Park, K.-Y., Kim, H., Kim, S.-W., and Kang, K. (2014). Aqueous rechargeable Li and Na ion batteries. *Chem. Rev.* 114, 11788–11827. doi: 10.1021/cr500232y
- Kim, H., Lee, J. T., Lee, D.-C., Oschatz, M., Cho, W. I., Kaskel, S., et al. (2013). Enhancing performance of Li-S cells using a Li-Al alloy anode coating. *Electrochem. Commun.* 36, 38–41. doi: 10.1016/j.elecom.2013.09.002
- Klayman, B., and Bernie, W. (2013). *Tesla Reports Third Fire Involving Model S Electric Car*. Reuters.
- Kong, L., Li, C., Jiang, J., and Pecht, M. G. (2018a). Li-ion battery fire hazards and safety strategies. *Energies* 11, 2191/1–2191/11. doi: 10.3390/en11092191
- Kong, L., Wang, Y., Yu, H., Liu, B., Qi, S., Wu, D., et al. (2018b). *In situ* armoring: a robust, high-wettability, and fire-resistant hybrid separator for advanced and safe batteries. *ACS Appl. Mater. Interfaces* 11, 2978–2988. doi: 10.1021/acsami.8b17521
- Kozen, A. C., Lin, C.-F., Pearse, A. J., Schroeder, M. A., Han, X., Hu, L., et al. (2015). Next-generation lithium metal anode engineering via atomic layer deposition. *ACS Nano* 9, 5884–5892. doi: 10.1021/acsnano.5b02166
- Kraysberg, A., and Ein-Eli, Y. (2012). Higher, stronger, better. A review of 5 volt cathode materials for advanced lithium-ion batteries. *Adv. Energy Mater.* 2, 922–939. doi: 10.1002/aenm.201200068
- Lazzari, M., and Scrosati, B. (1980). A cyclable lithium organic electrolyte cell based on two intercalation electrodes. *J. Electrochem. Soc.* 127, 773–4. doi: 10.1149/1.2129753
- Le Bideau, J., Viau, L., and Vioux, A. (2011). Ionogels, ionic liquid based hybrid materials. *Chem. Soc. Rev.* 40, 907–925. doi: 10.1039/C0CS00059K
- Lee, H., Ren, X., Niu, C., Yu, L., Engelhard, M. H., Cho, I., et al. (2017). Suppressing lithium dendrite growth by metallic coating on a separator. *Adv. Funct. Mater.* 27:1704391. doi: 10.1002/adfm.201704391
- Lee, Y. M., Kim, J.-W., Choi, N.-S., Lee, J. A., Seol, W.-H., and Park, J.-K. (2005). Novel porous separator based on PVdF and PE non-woven matrix for rechargeable lithium batteries. *J. Power Sources* 139, 235–241. doi: 10.1016/j.jpowsour.2004.06.055
- Li, S., and Church, B. C. (2017). Electrochemical stability of aluminum current collector in aqueous rechargeable lithium-ion battery electrolytes. *J. Appl. Electrochem.* 47, 839–853. doi: 10.1007/s10800-017-1081-2

- Li, W., Yao, H., Yan, K., Zheng, G., Liang, Z., Chiang, Y.-M., et al. (2015). The synergetic effect of lithium polysulfide and lithium nitrate to prevent lithium dendrite growth. *Nat. Commun.* 6:7436. doi: 10.1038/ncomms8436
- Li, X., Colclasure, A. M., Finegan, D. P., Ren, D., Shi, Y., Feng, X., et al. (2019). Degradation mechanisms of high capacity 18650 cells containing Si-graphite anode and nickel-rich NMC cathode. *Electrochim. Acta* 297, 1109–1120. doi: 10.1016/j.electacta.2018.11.194
- Li, Z., Xiong, Y., Sun, S., Zhang, L., Li, S., Liu, X., et al. (2018). Tri-layer nonwoven membrane with shutdown property and high robustness as a high-safety lithium ion battery separator. *J. Memb. Sci.* 565, 50–60. doi: 10.1016/j.memsci.2018.07.094
- Liang, Z., Zheng, G., Liu, C., Liu, N., Li, W., Yan, K., et al. (2015). Polymer nanofiber-guided uniform lithium deposition for battery electrodes. *Nano Lett.* 15, 2910–2916. doi: 10.1021/nl5046318
- Liao, H.-G., Zherebetskyy, D., Xin, H., Czarnik, C., Ercius, P., Elmlund, H., et al. (2014). Facet development during platinum nanocube growth. *Science* 345, 916–919. doi: 10.1126/science.1253149
- Liu, Y., Lin, D., Liang, Z., Zhao, J., Yan, K., and Cui, Y. (2016). Lithium-coated polymeric matrix as a minimum volume-change and dendrite-free lithium metal anode. *Nat. Commun.* 7:10992. doi: 10.1038/ncomms10992
- Lopez, C. F., Jeevarajan, J. A., and Mukherjee, P. P. (2015). Experimental analysis of thermal runaway and propagation in lithium-ion battery modules. *J. Electrochem. Soc.* 162, A1905–A1915. doi: 10.1149/2.0921509jes
- Loveridge, M. J., Remy, G., Kourra, N., Genieser, R., Barai, A., Lain, M. J., et al. (2018). Looking deeper into the galaxy (note 7). *Batteries* 4, 3/1–3/11. doi: 10.3390/batteries4010003
- Lu, L.-L., Ge, J., Yang, J.-N., Chen, S.-M., Yao, H.-B., Zhou, F., et al. (2016). Free-standing copper nanowire network current collector for improving lithium anode performance. *Nano Lett.* 16, 4431–4437. doi: 10.1021/acs.nanolett.6b01581
- Lu, Z., Liang, Q., Wang, B., Tao, Y., Zhao, Y., Lv, W., et al. (2019). Graphitic carbon nitride induced micro-electric field for dendrite-free lithium metal anodes. *Adv. Energy Mater.* 9:1803186. doi: 10.1002/aenm.201803186
- Mark, R. P. (2014). "NTSB issues recommendations on lithium-ion batteries," in *Aviation International News*. AINsafety.
- McCloskey, B. D. (2015). Attainable gravimetric and volumetric energy density of Li-S and Li ion battery cells with solid separator-protected Li metal anodes. *J. Phys. Chem. Lett.* 6, 4581–4588. doi: 10.1021/acs.jpclett.5b01814
- Mizushima, K., Jones, P. C., Wiseman, P. J., and Goodenough, J. B. (1980). Lithium cobalt oxide (Li<sub>x</sub>CoO<sub>2</sub>) (0 < x ≤ 1): a new cathode material for batteries of high energy density. *Mater. Res. Bull.* 15, 783–9. doi: 10.1016/0025-5408(80)90012-4
- Monroe, C., and Newman, J. (2005). The impact of elastic deformation on deposition kinetics at lithium/polymer interfaces. *J. Electrochem. Soc.* 152, A396–A404. doi: 10.1149/1.1850854
- Moreno, N., Caballero, A., Morales, J., and Rodriguez-Castellon, E. (2016). Improved performance of electrodes based on carbonized olive stones/S composites by impregnating with mesoporous TiO<sub>2</sub> for advanced Li-S batteries. *J. Power Sources* 313, 21–29. doi: 10.1016/j.jpowsour.2016.02.061
- Mukanova, A., Nurpeissova, A., Kim, S.-S., Myronov, M., and Bakenov, Z. (2018). N-type doped silicon thin film on a porous Cu Current collector as the negative electrode for li-ion batteries. *Chem. Open* 7, 92–96. doi: 10.1002/open.201700162
- Mukanova, A., Nurpeissova, A., Urazbayev, A., Kim, S.-S., Myronov, M., and Bakenov, Z. (2017). Silicon thin film on graphene coated nickel foam as an anode for Li-ion batteries. *Electrochim. Acta* 258, 800–806. doi: 10.1016/j.electacta.2017.11.129
- Mullins, W. W., and Sekerka, R. F. (1963). Morphological stability of a particle growing by diffusion or heat flow. *J. Appl. Phys.* 34, 323–9. doi: 10.1063/1.1702607
- Mun, J., Kim, S., Yim, T., Ryu, J. H., Kim, Y. G., and Oh, S. M. (2010). Comparative study on surface films from ionic liquids containing saturated and unsaturated substituent for LiCoO<sub>2</sub>. *J. Electrochem. Soc.* 157, A136–A141. doi: 10.1149/1.3265476
- Mun, J., Yim, T., Park, J. H., Ryu, J. H., Lee, S. Y., Kim, Y. G., et al. (2014). Allylic ionic liquid electrolyte-assisted electrochemical surface passivation of LiCoO<sub>2</sub> for advanced, safe lithium-ion batteries. *Sci. Rep.* 4:5802. doi: 10.1038/srep05802
- Nagasubramanian, G., and Fenton, K. (2013). Reducing Li-ion safety hazards through use of non-flammable solvents and recent work at Sandia National Laboratories. *Electrochim. Acta* 101, 3–10. doi: 10.1016/j.electacta.2012.09.065
- Nagasubramanian, G., and Orendorff, C. J. (2011). Hydrofluoroether electrolytes for lithium-ion batteries: reduced gas decomposition and nonflammable. *J. Power Sources* 196, 8604–8609. doi: 10.1016/j.jpowsour.2011.05.078
- Nishi, Y. (2001). The development of lithium ion secondary batteries. *Chem. Record* 1, 406–413. doi: 10.1002/tcr.1024
- Nunes-Pereira, J., Costa, C. M., Sousa, R. E., Machado, A. V., Silva, M. M., and Lanceros-Mendez, S. (2014). Li-ion battery separator membranes based on barium titanate and poly(vinylidene fluoride-co-trifluoroethylene): Filler size and concentration effects. *Electrochim. Acta* 117, 276–284. doi: 10.1016/j.electacta.2013.11.122
- Orendorff, C. J. (2012). The role of separators in lithium-ion cell safety. *Electrochem. Soc. Interface* 21, 61–65. doi: 10.1149/2.F07122if
- Ould Ely, T., Kamzabek, D., Chakraborty, D., and Doherty, M. F. (2018). Lithium-sulfur batteries: state of the art and future directions. *ACS Appl. Energy Mater.* 1, 1783–1814. doi: 10.1021/acsaem.7b00153
- Ould-Ely, T., Prieto-Centurion, D., Kumar, A., Guo, W., Knowles, W. V., Asokan, S., et al. (2006). Manganese(II) oxide nanohexapods: insight into controlling the form of nanocrystals. *Chem. Mater.* 18, 1821–1829. doi: 10.1021/cm052492q
- Park, K. H., Bai, Q., Kim, D. H., Oh, D. Y., Zhu, Y., Mo, Y., et al. (2018). Design strategies, practical considerations, and new solution processes of sulfide solid electrolytes for all-solid-state batteries. *Adv. Energy Mater.* 8:1800035. doi: 10.1002/aenm.201800035
- Pender, J. P., Xiao, H., Dong, Z., Cavallaro, K. A., Weeks, J. A., Heller, A., et al. (2019). Compact lithium-ion battery electrodes with lightweight reduced graphene oxide/poly(acrylic acid) current collectors. *ACS Appl. Energy Mater.* 2, 905–912. doi: 10.1021/acsaem.8b02007
- Pesaran, A. A., Kim, G.-H., and Smith, K. (2008). *Designing Safe Lithium-Ion Battery Packs Using Thermal Abuse Models*. Available online at: <https://www.nrel.gov/docs/fy09osti/45388.pdf>
- Porz, L., Swamy, T., Sheldon, B. W., Rettenwander, D., Froemling, T., Thaman, H. L., et al. (2017). Mechanism of lithium metal penetration through inorganic solid electrolytes. *Adv. Energy Mater.* 7:1701003. doi: 10.1002/aenm.201701003
- Quinzeni, I., Ferrari, S., Quartarone, E., Tomasi, C., Fagnoni, M., and Mustarelli, P. (2013). Li-doped mixtures of alkoxy-N-methylpyrrolidinium bis(trifluoromethanesulfonyl)-imide and organic carbonates as safe liquid electrolytes for lithium batteries. *J. Power Sources* 237, 204–209. doi: 10.1016/j.jpowsour.2013.03.036
- Roth, E. P., and Doughty, D. H. (2006). *Proceeding of AABC*, Baltimore, MD. Available online at: <https://www.nrel.gov/docs/fy13osti/54404.pdf> (accessed July 2019).
- Roth, E. P., Doughty, D. H., and Pile, D. L. (2007). Effects of separator breakdown on abuse response of 18650 Li-ion cells. *J. Power Sources* 174, 579–583. doi: 10.1016/j.jpowsour.2007.06.163
- Roth, E. P., and Orendorff, C. J. (2012). How electrolytes influence battery safety. *Electrochem. Soc. Interface* 21, 45–49. doi: 10.1149/2.F04122if
- Rusakova, I., Ould-Ely, T., Hofmann, C., Prieto-Centurion, D., Levin, C. S., Halas, N. J., et al. (2007). Nanoparticle shape conservation in the conversion of MnO nanocrystals into Mn<sub>3</sub>O<sub>4</sub>. *Chem. Mater.* 19, 1369–1375. doi: 10.1021/cm062649u
- Ryou, M.-H., Lee, Y. M., Park, J.-K., and Choi, J. W. (2011). Mussel-inspired polydopamine-treated polyethylene separators for high-power Li-Ion batteries. *Adv. Mater.* 23, 3066–3070. doi: 10.1002/adma.201100303
- Sanechika, K., and Yoshino, A. (1985). *Nonaqueous Secondary Battery*. Japanese Kokai Tokkyo Koho. JP Patent No. 60253157 A 19851213.
- Saw, L. H., Ye, Y., Yew, M. C., Chong, W. T., Yew, M. K., and Ng, T. C. (2017). Computational fluid dynamics simulation on open cell aluminium foams for Li-ion battery cooling system. *Appl. Energy* 204, 1489–1499. doi: 10.1016/j.apenergy.2017.04.022
- Schmuck, R., Wagner, R., Hoerpel, G., Placke, T., and Winter, M. (2018). Performance and cost of materials for lithium-based rechargeable automotive batteries. *Nat. Energy* 3, 267–278. doi: 10.1038/s41560-018-0107-2
- Sendek, A. D., Cubuk, E. D., Antoniuk, E. R., Cheon, G., Cui, Y., and Reed, E. J. (2018). Machine learning-assisted discovery of solid Li-Ion conducting materials. *Chem. Mater.* 31, 342–352. doi: 10.1021/acs.chemmater.8b03272

- Sharafi, A., Meyer, H. M., Nanda, J., Wolfenstine, J., and Sakamoto, J. (2016). Characterizing the Li-Li<sub>7</sub>La<sub>3</sub>Zr<sub>2</sub>O<sub>12</sub> interface stability and kinetics as a function of temperature and current density. *J. Power Sources* 302, 135–139. doi: 10.1016/j.jpowsour.2015.10.053
- Sharifi-Asl, S., Lu, J., Amine, K., and Shahbazian-Yassar, R. (2019). Oxygen release degradation in Li-Ion battery cathode materials: mechanisms and mitigating approaches. *Adv. Energy Mater.* 9:1900551. doi: 10.1002/aenm.201900551
- Shi, C., Dai, J., Li, C., Shen, X., Peng, L., Zhang, P., et al. (2017). A modified ceramic-coating separator with high-temperature stability for lithium-ion battery. *Polymers* 9, 159/1–159/12. doi: 10.3390/polym9050159
- Spotnitz, R. M., Weaver, J., Yeduvaka, G., Doughty, D. H., and Roth, E. P. (2007). Simulation of abuse tolerance of lithium-ion battery packs. *J. Power Sources* 163, 1080–1086. doi: 10.1016/j.jpowsour.2006.10.013
- Suo, L., Borodin, O., Gao, T., Olguin, M., Ho, J., Fan, X., et al. (2015). “Water-in-salt” electrolyte enables high-voltage aqueous lithium-ion chemistries. *Science* 350, 938–943. doi: 10.1126/science.aab1595
- Suo, L., Oh, D., Lin, Y., Zhuo, Z., Borodin, O., Gao, T., et al. (2017). How solid-electrolyte interphase forms in aqueous electrolytes. *J. Am. Chem. Soc.* 139, 18670–18680. doi: 10.1021/jacs.7b10688
- Swamy, T., Park, R., Sheldon, B. W., Rettenwander, D., Porz, L., Berendts, S., et al. (2018). Lithium metal penetration induced by electrodeposition through solid electrolytes: example in single-crystal Li<sub>6</sub>La<sub>3</sub>ZrTaO<sub>12</sub> garnet. *J. Electrochem. Soc.* 165, A3648–A3655. doi: 10.1149/2.1391814jes
- Taggougui, M., Diaw, M., Carre, B., Willmann, P., and Lemordant, D. (2008). Solvents in salt electrolyte: Benefits and possible use as electrolyte for lithium-ion battery. *Electrochim. Acta* 53, 5496–5502. doi: 10.1016/j.electacta.2008.03.012
- Tian, R., Wan, S., Guan, L., Duan, H., Guo, Y., Li, H., et al. (2018). Oriented growth of Li metal for stable Li/carbon composite negative electrode. *Electrochim. Acta* 292, 227–233. doi: 10.1016/j.electacta.2018.09.165
- Tsakamoto, H., Kishiyama, C., Nagata, M., Nakahara, H., and Piao, T. (2015). *Lithium Ion Battery Capable of Being Discharged to Zero Volts*. US Patent No. 20150074987 A1 20150319. U.S. Patent Application Public.
- Umh, H. N., Park, J., Yeo, J., Jung, S., Nam, I., and Yi, J. (2019). Lithium metal anode on a copper dendritic superstructure. *Electrochem. Commun.* 99, 27–31. doi: 10.1016/j.elecom.2018.12.015
- Wang, A., Kadam, S., Li, H., Shi, S., and Qi, Y. (2018). Review on modeling of the anode solid electrolyte interphase (SEI) for lithium-ion batteries. *NPJ Comput. Mater.* 4, 1–26. doi: 10.1038/s41524-018-0064-0
- Wang, L., Wang, Y., and Xia, Y. (2015). A high performance lithium-ion sulfur battery based on a Li<sub>2</sub>S cathode using a dual-phase electrolyte. *Energy Environ. Sci.* 8, 1551–1558. doi: 10.1039/C5EE00058K
- Wang, L., Yin, S., and Xu, J. (2019). A detailed computational model for cylindrical lithium-ion batteries under mechanical loading: from cell deformation to short-circuit onset. *J. Power Sources* 413, 284–292. doi: 10.1016/j.jpowsour.2018.12.059
- Wang, Q., Jiang, L., Yu, Y., and Sun, J. (2019). Progress of enhancing the safety of lithium ion battery from the electrolyte aspect. *Nano Energy* 55, 93–114. doi: 10.1016/j.nanoen.2018.10.035
- Wang, Q. S., Ping P., and Sun, J.H. (2010). Catastrophe analysis of cylindrical lithium ion battery. *Nonlinear Dynam.* 61, 63–772. doi: 10.1007/s11071-010-9685-7
- Wang, Q. S., Ping P., Zhao, X., Chu, G., Zhao, X., Sun, J.H., et al. (2012). Thermal runaway caused fire and explosion of lithium ion battery. *J. Power Sources* 208, 210–224. doi: 10.1016/j.jpowsour.2012.02.038
- Wei, M., Yuan, P., Chen, W., Hu, J., Mao, J., and Shao, G. (2015). Facile assembly of partly graphene-enveloped sulfur composites in double-solvent for lithium-sulfur batteries. *Electrochim. Acta* 178, 564–570. doi: 10.1016/j.electacta.2015.07.174
- Wongtharom, N., Lee, T.-C., Hsu, C.-H., Ting-Kuo Fey, G., Huang, K.-P., and Chang, J.-K. (2013). Electrochemical performance of rechargeable Li/LiFePO<sub>4</sub> cells with ionic liquid electrolyte: effects of Li salt at 25 °C and 50 °C. *J. Power Sources* 240, 676–682. doi: 10.1016/j.jpowsour.2013.05.014
- Wu, H., Zhuo, D., Kong, D., and Cui, Y. (2014). Improving battery safety by early detection of internal shorting with a bifunctional separator. *Nat. Commun.* 5:5193. doi: 10.1038/ncomms6193
- Xie, J., Liao, L., Gong, Y., Li, Y., Shi, F., Pei, A., et al. (2017). Stitching h-BN by atomic layer deposition of LiF as a stable interface for lithium metal anode. *Sci. Adv.* 3:eaa03170. doi: 10.1126/sciadv.aao3170
- Xiong, R., Li, L., and Tian, J. (2018). Towards a smarter battery management system: a critical review on battery state of health monitoring methods. *J. Power Sources* 405, 18–29. doi: 10.1016/j.jpowsour.2018.10.019
- Yan, K., Lu, Z., Lee, H.-W., Xiong, F., Hsu, P.-C., Li, Y., et al. (2016). Selective deposition and stable encapsulation of lithium through heterogeneous seeded growth. *Nat. Energy* 1:16010. doi: 10.1038/nenergy.2016.10
- Yang, C., Chen, J., Ji, X., Pollard, T. P., Lu, X., Sun, C.-J., et al. (2019). Aqueous Li-ion battery enabled by halogen conversion-intercalation chemistry in graphite. *Nature* 569, 245–250. doi: 10.1038/s41586-019-1175-6
- Yang, C., Fu, K., Zhang, Y., Hitz, E., and Hu, L. (2017a). Protected Lithium-metal anodes in batteries: from liquid to solid. *Adv. Mater.* 29:1701169. doi: 10.1002/adma.201701169
- Yang, C., Yao, Y., He, S., Xie, H., Hitz, E., and Hu, L. (2017b). Ultrafine silver nanoparticles for seeded lithium deposition toward stable lithium metal anode. *Adv. Mater.* 29:1702714. doi: 10.1002/adma.201702714
- Yao, X., Xie, S., Chen, C., Wang, Q., Sun, J., Li, Y., et al. (2005). Comparative study of trimethyl phosphite and trimethyl phosphate as electrolyte additives in lithium ion batteries. *J. Power Sources* 144, 170–175. doi: 10.1016/j.jpowsour.2004.11.042
- Yazami, R., and Touzain, P. (1983). A reversible graphite-lithium anode for batteries. *J. Power Sources* 9, 365–71. doi: 10.1016/0378-7753(83)87040-2
- Ye, M., Xiao, Y., Cheng, Z., Cui, L., Jiang, L., and Qu, L. (2018). A smart, anti-piercing and eliminating-dendrite lithium metal battery. *Nano Energy* 49, 403–410. doi: 10.1016/j.nanoen.2018.04.078
- Yim, T., Park, M.-S., Woo, S.-G., Kwon, H.-K., Yoo, J.-K., Jung, Y. S., et al. (2015). Self-extinguishing lithium ion batteries based on internally embedded fire-extinguishing microcapsules with temperature-responsiveness. *Nano Lett.* 15, 5059–5067. doi: 10.1021/acs.nanolett.5b01167
- Yoshino, A. (2012). The Birth of the Lithium-Ion Battery. *Angew. Chem. Int. Ed.* 51, 5798–5800. doi: 10.1002/anie.201105006
- Yu, S., and Siegel, D. J. (2018). Grain boundary softening: a potential mechanism for lithium metal penetration through stiff solid electrolytes. *ACS Appl. Mater. Interfaces* 10, 38151–38158. doi: 10.1021/acsami.8b17223
- Yue, Y., and Liang, H. (2018). 3D current collectors for lithium-ion batteries: a topical review. *Small Methods* 2, 1–20. doi: 10.1002/smt.201800056
- Zeng, Z., Jiang, X., Wu, B., Xiao, L., Ai, X., Yang, H., et al. (2014). Bis (2, 2, 2-trifluoroethyl) methylphosphonate: An Novel Flame-retardant Additive for Safe Lithium-ion Battery. *Electrochim. Acta* 129, 300–304. doi: 10.1016/j.electacta.2014.02.062
- Zhang, C., Lv, W., Zhou, G., Huang, Z., Zhang, Y., Lyu, R., et al. (2018). Vertically aligned lithiophilic CuO nanosheets on a Cu collector to stabilize lithium deposition for lithium metal batteries. *Adv. Energy Mater.* 8:1703404. doi: 10.1002/aenm.201703404
- Zhang, H., Liao, X., Guan, Y., Xiang, Y., Li, M., Zhang, W., et al. (2018). Lithiophilic-lithiophobic gradient interfacial layer for a highly stable lithium metal anode. *Nat. Commun.* 9, 1–11. doi: 10.1038/s41467-018-06126-z
- Zhang, S. S. (2007). A review on the separators of liquid electrolyte Li-ion batteries. *J. Power Sources* 164, 351–364. doi: 10.1016/j.jpowsour.2006.10.065
- Zhang, X.-Q., Chen, X., Hou, L.-P., Li, B.-Q., Cheng, X.-B., Huang, J.-Q., et al. (2019). Regulating anions in the solvation sheath of lithium ions for stable lithium metal batteries. *ACS Energy Lett.* 4, 411–416. doi: 10.1021/acscenergylett.8b02376
- Zhang, X.-Q., Chen, X., Xu, R., Cheng, X.-B., Peng, H.-J., Zhang, R., et al. (2017a). Columnar lithium metal anodes. *Angew. Chem. Int. Ed.* 56, 14207–14211. doi: 10.1002/anie.201707093
- Zhang, X.-Q., Cheng, X.-B., Chen, X., Yan, C., and Zhang, Q. (2017b). Fluoroethylene carbonate additives to render uniform Li deposits in lithium metal batteries. *Adv. Funct. Mater.* 27:1605989. doi: 10.1002/adfm.201605989
- Zheng, G., Lee, S. W., Liang, Z., Lee, H.-W., Yan, K., Yao, H., et al. (2014). Interconnected hollow carbon nanospheres for stable lithium metal anodes. *Nat. Nanotechnol.* 9, 618–623. doi: 10.1038/nnano.2014.152

- Zheng, J., Tang, M., and Hu, Y.-Y. (2016). Lithium ion pathway within  $\text{Li}_7\text{La}_3\text{Zr}_2\text{O}_{12}$ -polyethylene oxide composite electrolytes. *Angew. Chem. Int. Ed.* 55, 12538–12542. doi: 10.1002/anie.201607539
- Zhong, G., Li, H., Wang, C., Xu, K., and Wang, Q. (2018). Experimental analysis of thermal runaway propagation risk within 18650 lithium-ion battery modules. *J. Electrochem. Soc.* 165, A1925–A1934. doi: 10.1149/2.0461809jes
- Zhu, B., Jin, Y., Hu, X., Zheng, Q., Zhang, S., Wang, Q., et al. (2017). Poly(dimethylsiloxane) thin film as a stable interfacial layer for high-performance lithium-metal battery anodes. *Adv. Mater.* 29:1603755. doi: 10.1002/adma.201603755
- Zou, P., Wang, Y., Chiang, S.-W., Wang, X., Kang, F., and Yang, C. (2018). Directing lateral growth of lithium dendrites in micro-compartmented anode arrays for safe lithium metal batteries. *Nat. Commun.* 9, 1–9. doi: 10.1038/s41467-018-02888-8
- Conflict of Interest Statement:** The authors declare that the research was conducted in the absence of any commercial or financial relationships that could be construed as a potential conflict of interest.

*Copyright © 2019 Ould Ely, Kamzabek and Chakraborty. This is an open-access article distributed under the terms of the Creative Commons Attribution License (CC BY). The use, distribution or reproduction in other forums is permitted, provided the original author(s) and the copyright owner(s) are credited and that the original publication in this journal is cited, in accordance with accepted academic practice. No use, distribution or reproduction is permitted which does not comply with these terms.*